Batteries and Hydrogen Storage: Technical Analysis and Commercial Revision to Select the Best Option

José Manuel Andújar *[ID], Francisca Segura [ID], Jesús Rey [ID] and Francisco José Vivas [ID]

Research Centre CITES (Centro de Investigación en Tecnología, Energía y Sostenibilidad), Campus La Rábida, University of Huelva, Avenida de las Artes, 21007 Huelva, Spain
* Correspondence: andujar@diesia.uhu.es; Tel.: +34-959-217-380

Abstract: This paper aims to analyse two energy storage methods—batteries and hydrogen storage technologies—that in some cases are treated as complementary technologies, but in other ones they are considered opposed technologies. A detailed technical description of each technology will allow to understand the evolution of batteries and hydrogen storage technologies: batteries looking for higher energy capacity and lower maintenance, while hydrogen storage technologies pursuing better volumetric and gravimetric densities. Additionally, as energy storage systems, a mathematical model is required to know the state of charge of the system. For this purpose, a mathematical model is proposed for conventional batteries, for compressed hydrogen tanks, for liquid hydrogen storage and for metal hydride tanks, which makes it possible to integrate energy storage systems into management strategies that aim to solve the energy balance in plants based on hybrid energy storage systems. From the technical point of view, most batteries are easier to operate and do not require special operating conditions, while hydrogen storage methods are currently functioning at the two extremes (high temperatures for metal and complex hydrides and low temperatures for liquid hydrogen or physisorption). Additionally, the technical comparison made in this paper also includes research trends and future possibilities in an attempt to help plan future policies.

Keywords: energy storage; energy capacity; gravimetric and volumetric density; mathematical model; hydrogen storage method; battery; hydrogen; technical comparison

1. Introduction

It has long been accepted that the future of energy production will not rely on the fossil fuels used today, and the international scientific community is trying to find a sustainable solution to this problem [1,2]. However, production of energy is only half of the equation. How is energy demand guaranteed when production is lower than demand? How is it accessed safely and efficiently? For intermittent renewable energy sources (RES), such as wind and solar energy (which are mainly weather-dependent), it is vital to store the energy excess to be used in deficit situations [1].

Throughout the existence of humanity, there have been many different ways to store energy—from wood (to be burned) to batteries and from pseudocapacitors to hydrogen storage technologies [2]. Which one is the most useful? It often depends on its purpose, and on the consumer preferences. For example, some societies prefer gas stoves to electric ones because of the way food is cooked. Others prefer electric ones because the energy comes from a cleaner source. Then, regarding batteries and hydrogen, although batteries are suitable for small devices, because they can be made to whatever size is necessary, they are not a great option for mobility applications, due to the long recharging time (around hours), versus the few minutes needed by a hydrogen vehicle to be refuelled up.

On the other hand, it can be asserted that, in the conventional path of energy production, transmission and distribution, energy storage systems (ESS) are crucial, Figure 1.
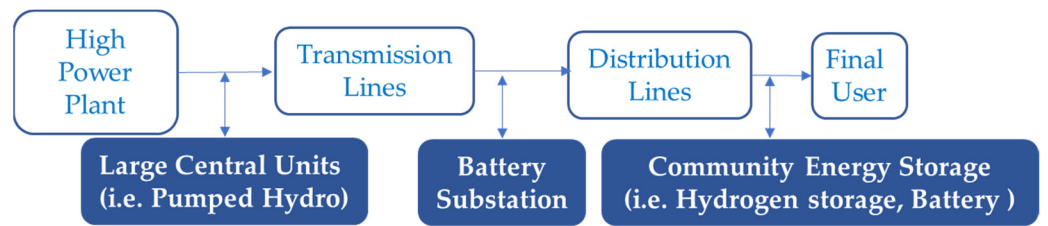
Figure 1. Conventional path of utility energy storage.

However, schemes of one-way power flow (with a centralised model) are becoming obsolete, contrary to the model of smart grid, more interactive for the consumers and easier to accommodate the ever-increasing number of ESS. Distributed generation systems, in which it is necessary a bidirectional relationship between customers and owners, are becoming more significant because customers are requesting for a better quality service (with a reduction of the number of blackouts) [3,4]. Those new systems, in which energy production takes place at points close to the place where the energy is consumed, are an opportunity to achieve greater integration of different ESS. Figures 2 and 3 present a classification of different ESS based on nature and mature of technology, respectively.
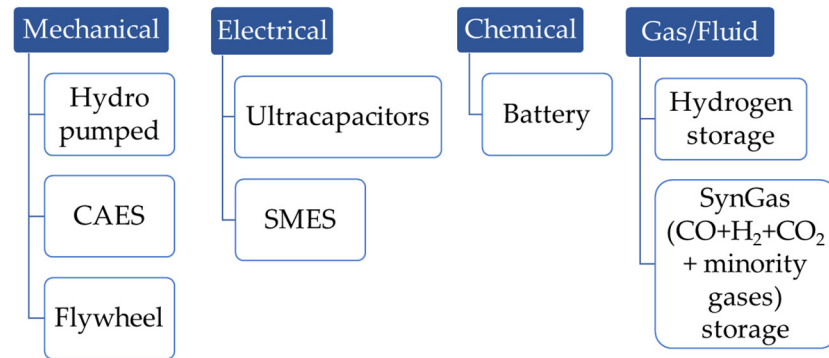

Figure 2. Energy Storage Technologies: Classification according to nature of technology. CAES: Compressed Air Energy Storage. SMES: Superconducting Magnetic Energy Storage.
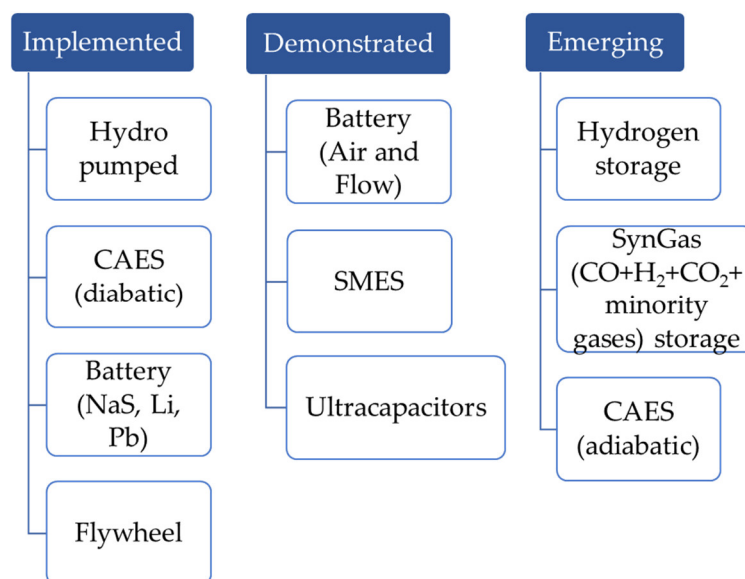

Figure 3. Energy Storage Technologies: Classification according to mature technology.

The choice of the best ESS will depend on the service that is being looked for, because each technology has unique properties that make it optimal for certain services [5]. Table 1 shows the advantages and drawbacks of the different ESS presented in Figures 2 and 3.

Table 1. Advantages and drawbacks of different ESS.

Technology	Advantages	Drawbacks
Hydro pumped [6]	- Low operating costs per energy unit. - Available for long-term storage. - Fast response. - High energy storage capacity.	- Very high investment costs. - Environmental issues. - Geographical and topographical limitations.
CAES [6]	- Large energy storage capacity. - High lifetime. - Lower cost per kW than hydro pumped.	- Originally, non-environmentally friendly. - Geographical restrictions to select underground reservoirs where the air is pressurised.
Ultracapacitors [6,7]	- High efficiency. - Low environmental impact. - High lifetime. - Medium capacity of storage. - High specific power. - Used in grid systems to stabilise them during peak demands.	- High costs. - Low specific energy.
Flywheels [6]	- Environmentally friendly. - High power and specific energy. - Low maintenance cost. - High life span. - High efficiency (85–90%). - No temperature control needed.	- High costs. - Short discharge time. - Low specific energy. - Mechanical stress and fatigue.
SMES [6]	- High efficiency (~95%). - High power capacity. - Environmentally friendly. - Fast response time.	- Need of continuous cooling. - High investment and operation costs. - Temperature sensitive.
SynGas storage ($CO+H_2+CO_2$ + minority gases) [8]	- Key role in reducing greenhouse gas emissions if carbon capture is included in reforming process. - High specific energy.	- Low volumetric density. - High costs. - Restricted to stationary applications.
Batteries [6]	- Widely used. - Can be used in devices of different sizes (from mobile phones to electric vehicles).	- Slow charging process. - Low specific energy.
Hydrogen storage [9]	- Hydrogen produced via renewable powered electrolysis plays a key role for greenhouse gas reduction. - High specific energy. - Quick charging process.	- Low volumetric density. - Variable gravimetric density, depending on the storage option.

According to Figure 1, both battery and hydrogen storage systems are two feasible options for energy storage at the connection point closest to the customer. This article presents a technical study of current technologies involving batteries and hydrogen storage systems and their uses in the market in an attempt to better understand the path their future developments should take. Then, conventional, molten salt, redox flow and metal-air battery technologies are studied; while regarding hydrogen storage systems, solutions based on compressed hydrogen, liquid hydrogen and metal hydrides storage are analysed in the paper.

The main contributions of the paper are listed below:

- A detailed study of battery and hydrogen storage technologies. The study includes fundamental principles of operation, classification and degree of technological maturity.
- A mathematical model for each technology, that allows to know the state of charge of the storage system in real time. In this way, it is possible to address energy management strategies in plants that combine storage systems of different nature such as hydrogen storage systems and battery systems.
- A technical analysis of all the studied technologies that allows to understand research trends and future possibilities in an attempt to aid in planning deciding policies.

2. Storage in Batteries. As Many Advantages as Varieties

There are two basic types of batteries: primary and secondary. The first one is not rechargeable, while the second one is. According to scientific records, the first battery was invented in 1799 by Alessandro Volta, who reported his invention to the Royal Society in London in 1800 [10]. However, the first rechargeable battery, based on lead-acid chemistry, was not discovered until 1860 by Gaston Planté [11]. This battery and those developed later contained a liquid electrolyte. It was not until 1881 that the first commercially successful dry cell battery was developed by Carl Gassner [12]. Next battery to be invented was the Nickel-Cadmium battery (by the Swedish Chemist Waldemar Jungner in 1899) [12], which used caustic KOH as its electrolyte. Many of these systems are still at the core of commercially available batteries today—most single use batteries, are based on the alkaline dry cell that Gassner originally invented [12].

After this, there have been appearing successively new designs which give name to the different technologies. Then, apart from conventional batteries, it is possible to find Molten Salt, Redox Flow and the most recent technology, Metal Air batteries, Figure 4.
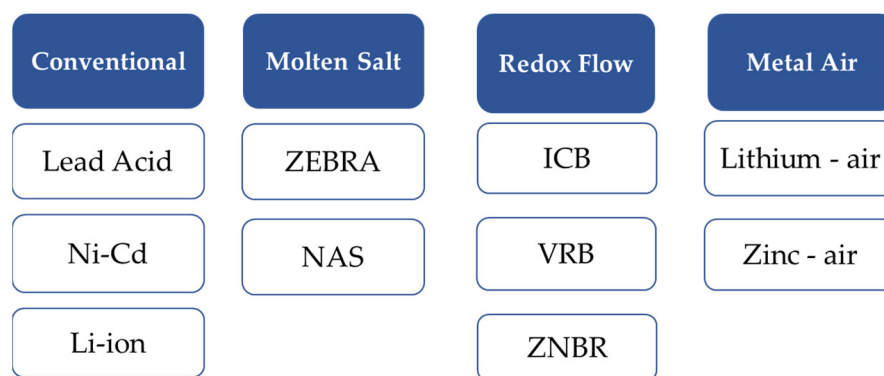
Conventional	Molten Salt	Redox Flow	Metal Air
Lead Acid	ZEBRA	ICB	Lithium - air
Ni-Cd	NAS	VRB	Zinc - air
Li-ion		ZNBR	

Figure 4. General classification of battery technologies.

The apparition of new types of batteries has led to the use of new terms. Then, the term *battery* refers to storage devices where the energy carrier is the electrode, the term *flow battery* is used when the energy carrier is the electrolyte and the term *fuel cell* involves devices where the energy carrier is the fuel (whose chemical energy is converted into electrical energy) [13]. However, some terms can lead to confusion. In this sense, scientific references, such as [14], consider metal/air batteries to be a hybrid between batteries and fuel cells (more specifically, the air cathode battery is considered a fuel cell). Next, a detailed study of existing battery technologies will help to understand their features and potential applications.

2.1. Conventional Technology

2.1.1. Fundamental Principles

Batteries included in this group are the most common and the most extended in the market, such as Lead-Acid, Nickel-Cadmium (Ni-Cd) and Lithium-ion (Li-ion) batteries. All of them have in common a redox reaction in which one of the electrodes releases electrons, which are used to supply the load in the external circuit and, after that, are carried to the other electrode. The electrode that releases electrons becomes positively charged (and will release cations to the other electrode through the electrolyte), while the electrode that receives electrons becomes negatively charged (and will release anions to the other electrode through the electrolyte), Figure 5, [15,16].
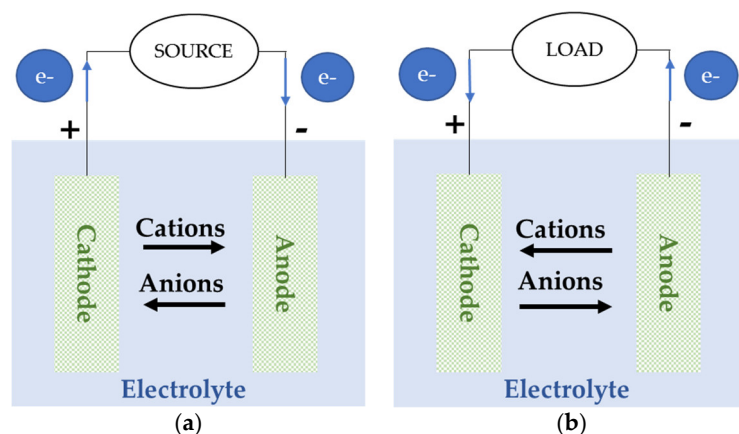
Figure 5. Cell configuration of a conventional battery during: (**a**) charge, (**b**) discharge.

The chemical characteristics and some manufacturers of the three types of batteries that have a cell configuration similar to this conventional design are shown in Table 2.

Table 2. Conventional batteries. Characteristics and Manufacturers.

Battery	Cell Reaction	Manufacturer
Lead-Acid	Anode: $Pb + HSO_4^- \rightleftharpoons 4Pb(II)SO_4 + H^+ + 2e^-$ Cathode: $Pb(IV)O_2 + 3H^+ + HSO_4^- + 2e^- \rightleftharpoons Pb(II)SO_4 + 2H_2O$ Overall cell: $PbO_2 + Pb + 2H_2SO_4 \rightleftharpoons 2PbSO_4 + 2H_2O$	MK Powered (Anaheim, USA), Exide (Milton, USA), Electro source (Canada), Clarios (Milwaukee, USA), Leoch (China) [17,18]
NiCd	Anode: $Cd + 2OH^- \rightleftharpoons Cd(OH)_2 + 2e^-$ Cathode: $2NiO(OH) + 2H_2O + 2e^- \rightleftharpoons 2Ni(OH)_2 + 2OH^-$ Overall cell: $2NiO(OH) + Cd + 2H_2O \rightleftharpoons 2Ni(OH)_2 + Cd(OH)_2$	SAFT (France), ALCAD (Irun, Spain), Raytalk (China), Enersys (Reading, USA), Mouser (Mansfield, USA), HAWKER GmbH (Germany), GAZ (Russia) [18–21]
Li-ion	Anode: $Li_xC_6 \rightleftharpoons xLi^+ + C_6 + xe^-$ Cathode: $Li_{1-x}XXO_2 + xLi^+ + xe^- \rightleftharpoons LiXXO_2$ Overall cell: $Li_xC_6 + Li_{1-x}XXO_2 \rightleftharpoons LiXXO_2 + C_6$	Panasonic (Osaka, Japan), LG Chem, SK Innovation (Seoul, South Korea), A123 Systems (Michigan, USA), Samsung SDI (Yongin, South Korea), CATL (Ningde, China), Toshiba (Tokyo, Japan), AESC (China), Bisco (Anaheim, USA) [18,22]

Rechargeable lead-acid battery was invented in 1860 [23,24] by the French scientist Gaston Planté, by comparing different large lead sheet electrodes (like silver, gold, platinum or lead electrodes) immersed in diluted aqueous sulfuric acid; experiment from which it was obtained that in a cell with lead electrodes immersed in the acid, the secondary current that flowed through it was the highest and flowed for the longest period of time. Although that first battery did not have a large capacity, it attracted the interest of scientists such as Fauré (who coated lead plates with a paste of water, sulfuric acid and red lead oxide), Volckmar (who replaced the lead sheet with a lead grid) or Sellon (who used lead-antimony grids instead of pure lead grids), so the capacity of these batteries was increased. Nowadays, as a result of the rapid development of the automobile after Second World War, which led to an exponential increase in the production of lead-acid batteries, these are used in various vehicles such as aircraft, submarines or hybrid electric vehicles. Nevertheless, these batteries are still under study and present different challenges such as increasing their power performance or their specific energy [23,24].

On the other hand, the rechargeable Nickel-cadmium (NiCd) battery was created in 1899 by the Swedish chemist Waldemar Jungner. Compared to lead-acid batteries, this battery has drawbacks such as its high initial cost. However, it has other advantages over lead-acid battery such as a lower maintenance, due to higher corrosion resistance [25]. This battery is currently used for portable electronics applications, but one of its major

drawbacks is that it is made of toxic materials, so proper management and recycling of those materials is a current challenge for this technology [26].

As for the last group of conventional batteries, experiments for lithium-ion batteries began in 1912, but it was not until 1980 that John B. Goodenough created rechargeable lithium-ion batteries, such as those used in electronic devices around the world [27,28]. Lithium-ion batteries replaced zinc-mercury batteries used up to the moment in medical devices, such as pacemakers, extending the replacement time from two to five years, and improving the survival rate from 75% to 100% [29].

2.1.2. Mathematical Model

Considering charge and discharge models for conventional batteries, in the battery model described by Tremblay et al. (that can be used for lead-acid, NiCd, lithium-ion and nickel-metal hydride batteries, for both charge and discharge cycles), the controlled voltage source is described by Equation (1) [30]:

$$V = V_0 - K \cdot \frac{Q}{Q - \int idt} - R_{elec}i + Ae^{-B \int idt} \tag{1}$$

where:
V: battery voltage (V)
V_0: no-load battery voltage (V)
K: polarization voltage (V)
Q: battery capacity (Ah)
R_{elec}: internal resistance (Ω)
i: battery current (A)
A: exponential zone amplitude (V)
B: inverse of the charge at the end of the exponential zone $(\text{Ah})^{-1}$.

In an attempt to obtain the mathematical model based on experimental data, it is first necessary to know V_0, K, A and B. In Figure 6, it is possible to identify the indicated points and obtain their values [30]. With the points in Figure 6 identified, previous parameters will be calculated thanks to Equations (2)–(5).
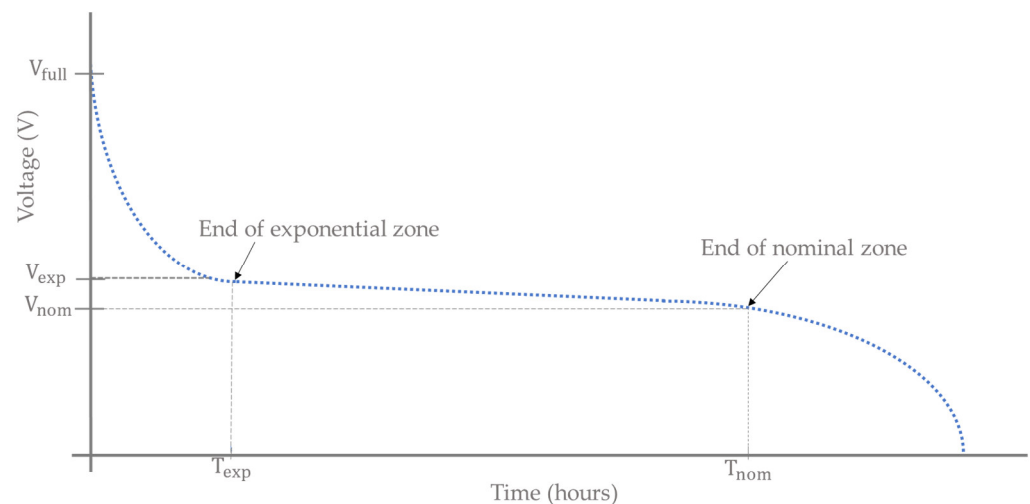

Figure 6. Typical conventional battery discharge curve.

$$A = V_{full} - V_{exp} \tag{2}$$

$$B = \frac{3}{Q_{exp}} \tag{3}$$

$$K = \frac{\left(V_{full} - V_{NOM} + A\left(e^{-BQ_{NOM}} - 1\right)\right)(Q - Q_{NOM})}{Q_{NOM}} \qquad (4)$$

$$V_0 = V_{full} + K + R_{elec}i - A \qquad (5)$$

where:

V_{full}: fully charged battery voltage (V)

V_{exp}: voltage at the end of exponential zone (V)

Q_{exp}: battery capacity at the end of exponential zone (Ah)

V_{NOM}: voltage at the end of nominal zone (V)

Q_{NOM}: battery capacity at the end of nominal zone (Ah).

Based on the above, Table 3 shows the typical parameters values for each of the conventional battery types studied in this paper [30]:

Table 3. Conventional batteries-controlled voltage source parameters.

Battery Parameter	Lead-Acid (12 V, 1.2 Ah)	NiCd (1.2 V, 1.3 Ah)	Li-Ion Polymer Battery (3.6 V, 1 Ah)
V_0 (V)	12.65	1.25	3.73
R (Ω)	0.25	0.023	0.09
K (V)	0.33	0.0085	0.0088
A (V)	0.66	0.14	0.47
B $(\text{Ah})^{-1}$	2884.61	5.77	3.53

2.1.3. Technical Comparison

Currently, the battery industry relies on lithium for its most efficient batteries, but this element is expensive and geographically unsustainable, as most of the current lithium mines are not in ideal locations for the US or Europe. This may be the reason why sodium batteries (see Section 2.2) are slowly being developed to have the same energy capacity as their lithium counterparts, as these batteries are much cheaper, and the required sodium can simply be extracted from the ocean or practically anywhere, given that it is the sixth most common element in the Earth's crust [31].

In the beginning, lithium batteries were tested out with a bunch of different cathodes, before settling on the first commercial cathode: magnesium dioxide. Now that both anode and cathode materials have reached a plateau of sorts, the challenge is to further improve the specific energy of batteries and make them more affordable, which will require a lot of effort [32].

From a technical point of view, Li-ion batteries can reach a high lifetime of 1000–10,000 cycles [2,33], ~8000 cycles [34], ~10,000 cycles [35], while NiCd batteries can reach a lifetime of >2000 cycles [2], 2000–2500 cycles [33,35] and, on the other hand, lead-acid batteries can only reach a lifetime of 500–1500 cycles [33], <2000 cycles [34], ~2500 cycles [35]; Li-ion batteries have the greatest specific energy (80–200 Wh/kg [2], 75–200 Wh/kg [33,34], ~200 Wh/kg [35], 100–265 Wh/kg [36]), compared to lead-acid batteries (30–50 Wh/kg [33], ~50 Wh/kg [35], 30–40 Wh/kg [36]) and NiCd batteries (50–75 Wh/kg [2,36], 45–80 Wh/kg [33], 55–75 Wh/kg [35]); and Li-ion batteries exhibit higher average round-trip efficiency (<97% [2], 85–95% [33], 90–95% [34,37], 85–90% [35], 92–95% [36]) than lead-acid batteries (80% [2], 60–95% [33], ~80% [34], 80–82% [36], 70–90% [37]) and NiCd batteries (60–91% [33], 72% [36]). Furthermore, Li-ion batteries have higher specific power (500–2000 W/kg [2], 400–1200 W/kg [33], 150–3000 W/kg [37]) than Ni-Cd batteries (150–300 W/kg [33]) and lead-acid batteries (75–300 W/kg [33,37]); and for Li-ion batteries a wider power range can be found (0–50 MW [33], 0–100 MW [37] for Li-ion batteries, compared to 0–40 MW [33] for NiCd batteries and 0–20 MW [33], 0–40 MW [37] for lead-acid batteries) although these three batteries can have a wide power range. Regarding the possible applications of conventional batteries, for lead-acid batteries applications such as household Uninterruptible Power Supply (UPS) of the order of few Wh or such as submarine power or load-levelling of the order of sev-

eral MWh can be found [38], while for Li-ion batteries applications such as portable electronic devices or electric vehicles (EVs) can be found [39] and finally for NiCd batteries applications such as aviation safety, telecommunication network or off-grid PV can be found [40].

Table 4 shows a summary of a technical comparison between the different conventional batteries.

Table 4. Comparison of the main technical parameters of the different conventional batteries.

Parameters	Lead-Acid	Li-Ion	NiCd
Efficiency (%)	60–95	85–97	60–91
Life cycles	500–2500	1000–10,000	2000–2500
Specific energy (Wh/kg)	30–50	75–265	45–80

Table A1 from Appendix A.1 shows different commercial models for each kind of conventional batteries.

2.2. Molten Salt Batteries

2.2.1. Fundamental Principles

Molten salt batteries (ZEBRA batteries and sodium sulphur batteries) are designed to take advantage of the conductivity of sodium ions, higher than 0.2 S/cm at 260 °C and with a positive temperature gradient. Consequently, they are used in applications where the temperature varies between 270 °C and 350 °C. As for the history of molten salt batteries, ZEBRA batteries were invented in South Africa and were first applied in 1978. For two decades, it was developed by Daimler-Chrysler and its current production depends on MES-DEA [41]. A few years after the appearance of ZEBRA, in 1983, Tokyo Electric Power Company (TEPCO) and NGK Insulators, Ltd. introduced sodium sulphur (NAS) batteries [42].

Both batteries proposals share the cylindrical design which characterizes this kind of batteries and, in both of them, a ceramic electrolyte made from β-Al_2O_3 (alumina) transfers the sodium ions between the positive and negative electrodes, Figure 7. In this kind of batteries, there is no side reaction, so there is no charge loss due to the ceramic electrolyte and, consequently, their efficiency is high.

The two mentioned proposals can be used in different energy storage applications such as electric vehicles [41,42]; however, both present a series of disadvantages that are a challenge for the development of both technologies. In the case of ZEBRA batteries, due to the high operation temperature, the development of ZEBRA batteries for automotive applications has been affected, since they present self-discharge issues. In this sense, the combination of ZEBRA batteries with Electrochemical Double Layer Capacitors (EDLCs) is being studied as a possible solution [43]. On the other hand, NAS battery also presents a high operation temperature that reduces its efficiency, moreover, the solid electrolyte can become brittle and break during operation, which can result in an increased risk of fire and explosion due to the penetration of molten sodium through the cell. In this sense, the use of a ceramic electrolyte and molten electrodes in this kind of batteries presents different challenges such as increasing the safety of their operation or reducing their operating temperature, which limit the applications of this technology [44].

Despite their drawbacks, these kinds of batteries have lifetime and specific energy three and four times respectively, as higher as conventional batteries. In addition, they can provide power peaks in less than 30 s, so they are used in applications where the quality of the power supply is the main decision factor.
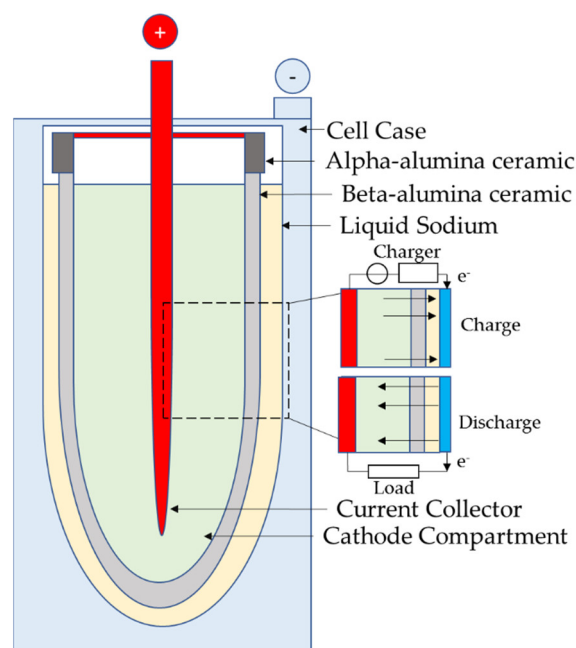
Figure 7. Cell configuration of molten salt batteries.

2.2.2. Technical Comparison

From a technical point of view, ZEBRA batteries can reach a lifetime from 2600 cycles [35] to 4000 cycles [45], while NAS batteries can reach a lifetime of 2500–4000 cycles [33], 2500–4500 cycles [35,37]; both batteries have similar operating temperature (265–350 °C [45], 270–350 °C [35] for ZEBRA batteries and 250–350 °C [2], 300–350 °C [46] for NAS batteries) and high specific energy that is higher for NAS batteries (150–240 Wh/kg [2,33], 100–240 Wh/kg [37]) than for ZEBRA batteries (approximately 100–120 Wh/kg [40,45]). However, NAS batteries have a higher round-trip efficiency than ZEBRA batteries (80–90% [2], 75–90% [33], 75–85% [35,37] vs. 70.7–80.9% [45]). On the other hand, NAS batteries present slightly higher specific power (150–230 W/kg [2], 100–230 W/kg [37]) than ZEBRA batteries (150–200 W/kg [2]). Regarding the applications of these types of batteries, ZEBRA batteries can be used in electric and hybrid electric vehicles or energy storage applications, while NAS batteries can be used for wind power integration or high-value grid services [46].

The main features of this kind of batteries are shown in Table 5, while a summary of a technical comparison between the different molten salt batteries is shown in Table 6. Table A2 in Appendix A.2 shows molten salt batteries models.

Table 5. Molten Salt batteries. Characteristics and manufacturers.

Battery	Cell Reaction	Manufacturer
ZEBRA	Anode: Molten sodium (Na) Cathode: Ni and NaCl impregnated with $NaAlCl_4$ Overall cell: $NaAlCl_4 + 3Na \rightleftharpoons 4NaCl + Al$	MES-DEA (Switzerland), Eurobat (Brussels, Belgium), FIAMM Sonick (Switzerland), General Electric (Boston, USA) [18,41]
NAS	Anode: Sodium (Na) Cathode: Sulfur (S) Overall cell: $2Na + xS \rightleftharpoons Na_2S_x$	NGK Insulators (Tokyo, Japan), ABB (Zürich, Switzerland), Silent Power (Switzerland), BASF (Ludwigshafen am Rhein, Germany) [18,42]

Table 6. Comparison of the main technical parameters of the different molten salt batteries.

Parameters	ZEBRA	NAS
Efficiency (%)	70.7–80.9	75–90
Life cycles	2600–4000	2500–4500
Specific energy (Wh/kg)	100–120	100–240

2.3. Redox Flow Batteries

2.3.1. Fundamental Principles

The two groups of batteries presented so far have well-defined applications based on their cell structure (conventional batteries for portable applications and molten salt batteries for applications requiring high quality power supply).

Nevertheless, none of these previous batteries accomplishes the requirements of the large-scale grid. First, at the grid connection line (a huge physical infrastructure, with almost no storage capability) grid storage is vital because it must uncouple oscillating customer demand from generation, which has a clear fluctuating character in the case of renewable energy sources.

Additionally, grid storage must be able to separate power from energy, tolerate a high number of charge/discharge cycles, to have good round-trip efficiency, to exhibit fast response to load or input changes, and all at reasonable capital costs [47].

Based on the above, a new cell design (Redox Flow Batteries, RFBs are also called *Regenerative Fuel Cells*, RFBs) was thought of where the reactants are not stored inside the electrode itself (as in previous battery designs), but are dissolved in the electrolyte solution and stored in external tanks, Figure 8, [48]. Then, additional balance-of-plant devices (pump, level sensors, etc.) are needed to make the liquid electrolyte flow. In addition, an Ion Exchange Membrane (IEM) separates the anolyte and catholyte solutions and allows for the transport of charge-carrying species. Furthermore, the IEM can act as an effective barrier to prevent permeation of active species and improve the ionic selectivity of the system by reducing the crosstalk of active species and addressing important drawbacks such as self-discharge or loss of capacity [49].
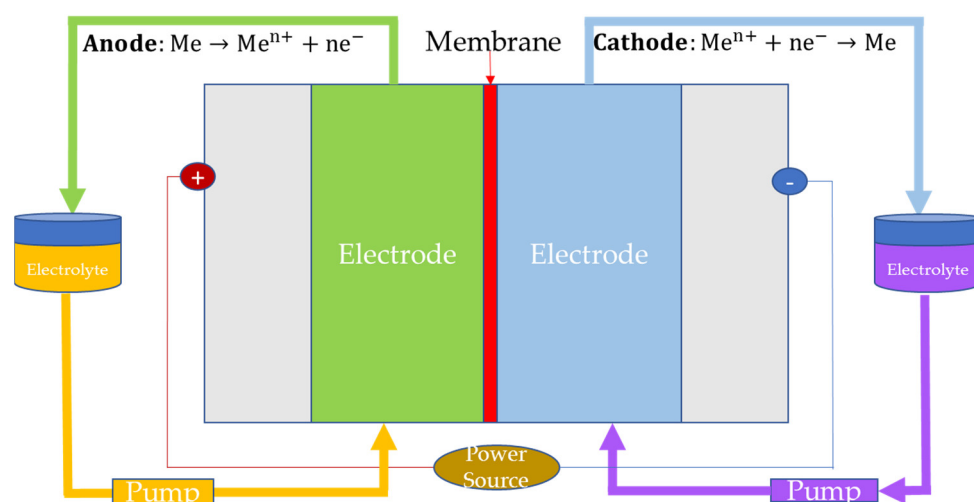

Anode: $Me \rightarrow Me^{n+} + ne^-$ Membrane   **Cathode**: $Me^{n+} + ne^- \rightarrow Me$

Figure 8. Cell configuration of redox flow batteries ("Me" refers to reactant dissolved in the electrolyte solution).

Additionally, thanks to the fact that there is no physical transfer of material across the electrode/electrolyte interface, the lifetime of this type of batteries is not directly influenced by the depth-of-discharge (DOD), as it is the case in conventional rechargeable batteries. In this type of batteries, the power is determined by the number of stacked cells and the stored energy depends on the reactants: their nature, their concentration, and the size of

tanks. In addition, for one of the batteries of this technology (Zinc Bromide battery), one of the potential risks is the formation of zinc dendrites, which will start their growth if the critical potential value is reached (at that moment, the equilibrium state will be broken and the growth of zinc dendrites will start). Furthermore, the growth of zinc dendrites will be accelerated in case the current density at the electrode surface is high and non-uniform [50].

There are three different electrolytes that form the basis of existing flow batteries designs, currently in demonstration or in development of large-scale projects, which are: Iron-Chromium (IC), Vanadium (VRB) and Zinc Bromide (ZNBR). Within the ZNBR batteries, it is possible to find other variants such as Polysulphide Bromide (PSB), in which the role played by zinc in the anode side is replaced by polysulphide.

The main features of the three types of batteries classified as RFB are shown in Table 7.

Table 7. Redox Flow Batteries. Characteristics and manufacturers.

Battery	Cell Reaction	Manufacturer/Developer
ICB	Anode: $Cr^{2+} \rightleftharpoons Cr^{3+} + 1e^-$ Cathode: $Fe^{3+} + 1e^- \rightleftharpoons Fe^{2+}$	NASA (Washington D.C., USA), Mitsui Engineering & Shipbuilding Co. Ltd. (Tokyo, Japan), Sumitomo Electric Industries Ltd. (Osaka, Japan) [51]
VRB	Anode: $V^{4+} \rightleftharpoons V^{5+} + 1e^-$ Cathode: $V^{3+} + 1e^- \rightleftharpoons V^{2+}$	University of South Wales (Cardiff, U.K.), UniEnergy Technologies (Mukilteo, USA), Rongke Power (Dalian, China), Kashima-Kita Electric Power Group (Japan), Kansai Electric Company (Osaka, Japan), Hokkaido Electric Power Company (Sapporo, Japan), Fraunhofer Institute (Münich, Germany), Sumitomo Electric Industries, Mitsubishi Chemicals (Tokyo, Japan) [51–53]
ZNBR	Anode: $Zn \rightleftharpoons Zn^{2+} + 2e^-$ Cathode: $Br_2 + 2e^- \rightleftharpoons 2Br^-$	RedFlow (Brisbane, Australia), Jofemar Energy (Peralta, Spain) [54,55]

As for the history of RFBs, ICBs were pioneered and studied extensively by NASA in the 70′s–80′s and by Mitsui in Japan [56]. However, the conceptual design of flow batteries was introduced in 1933 in a patent by Pissoort, who described the use of a vanadium redox couple. In the late 1970s, NASA studied flow batteries and considered the Fe-Cr and Fe-Ti redox pair to be the most promising systems. Later, in 1978, Pellegri and Spaziante patented the idea of using vanadium redox salts (without relevant developments), but it was not until 1986 that a group of Australian scientists at the University of New South Wales led by Skyllas-Kazacos achieved the first successful demonstration of a commercial vanadium cell, followed in 1989 by the development of vanadium redox batteries. As for ZNBR batteries, their concept appeared more than a hundred years ago; however, it was not until 1970–1980 when Exxon and Gould brought the first proposals to practical use [52].

2.3.2. Technical Comparison

From a technical point of view, ZNBRs present the highest specific energy (30–85 Wh/L [2], 30–60 Wh/L [37], 30–50 Wh/kg [33,37]) compared to VRBs (10–50 Wh/kg [2], 10–35 Wh/kg [33], 10–30 Wh/kg [37], 20–70 Wh/L [37]) and ICBs (15.8 Wh/L [41]); ICBs present lower round-trip efficiency (76.3–79.6% [57]) than VRBs (75–85% [2], 85–90% [33], 65–85% [37]) and slightly higher than ZNBRs (65–70% [2], 65–85% [33], 60–65 % [35], 70–80% [37]) and a higher operating temperature (40–60 °C) than VRBs and ZNBRs (10–40 °C) [52,58]. Finally, redox flow batteries present a high lifetime: 10,000–16,000 cycles [2], 12,000–18,000 cycles [33], >13,000 cycles [35], 10,000–13,000 cycles [37] for VRBs and >2000 cycles [33], 2000–10,000 cycles [37] for ZNBRs. Regarding the applications of these batteries, examples can be found such as UPS, interseasonal storage, load levelling function or electric and hybrid vehicles, especially those of large dimensions

(due to the low specific energy) [53]. Table 8 shows a summary of a technical comparison between the different RFBs.

Concerning current trends in redox flow batteries, RFBs can be found to present challenges such as research on the flow management and parameter estimation [53]. Furthermore, the possibility of modifying VRB systems in order to increase the density of the active material and, above all, to find replacements for vanadium, a relatively rare material, is currently being studied [52]. Another challenge faced by redox flow batteries are the limitations associated with IEMs, such as their high costs, safety concerns due to the evolution of toxic intermediates, or temperature limitations due to corrosive gases released at temperatures above 150 °C [59].

Table 8. Comparison of the main technical parameters of the different RFBs.

Parameters	ICB	VRB	ZNBR
Efficiency (%)	76.3–79.6	65–90	60–85
Life cycles	-	100,000–18,000	2000–10,000
Specific energy	15.8 Wh/L	20–70 Wh/L 10–50 Wh/kg	30–85 Wh/L 30–50 Wh/kg

Table A3 in Appendix A.3 shows different commercial models of redox flow batteries.

2.4. Metal-Air Batteries

2.4.1. Fundamental Principles

In order to achieve batteries with higher specific energy and lower maintenance than conventional rechargeable batteries, metal-air batteries were developed. These batteries have an open cell structure, i.e., on the one side the electrode is a metal (lithium or zinc) and, on the other side, the electrode is oxygen (regarding the different designs of the cell structures studied along the paper, this last group of metal-air batteries have a cell design that likely approach to fuel cells design), taken from the air, for the reaction to take place. Air is introduced through a channels-based structure and a catalyst ensures oxygen reduction. The intermediate electrolyte allows the flow of ions, and its nature establishes the type of battery: aqueous, non-aqueous, hybrid and solid-state metal–air batteries. In the case of aqueous and hybrid electrolyte, a metal ion conducting polymer membrane is required [60]. The configuration of the different metal–air batteries is shown in Figure 9. Although, there are primary (non-rechargeable) metal–air batteries, such as aluminium–air (Al-air) or magnesium–air (Mg–air) batteries, our study will be focused on secondary (rechargeable) batteries: lithium–air (Li–air) and zinc–air batteries (Zn–air) [61] as shown in Table 9.
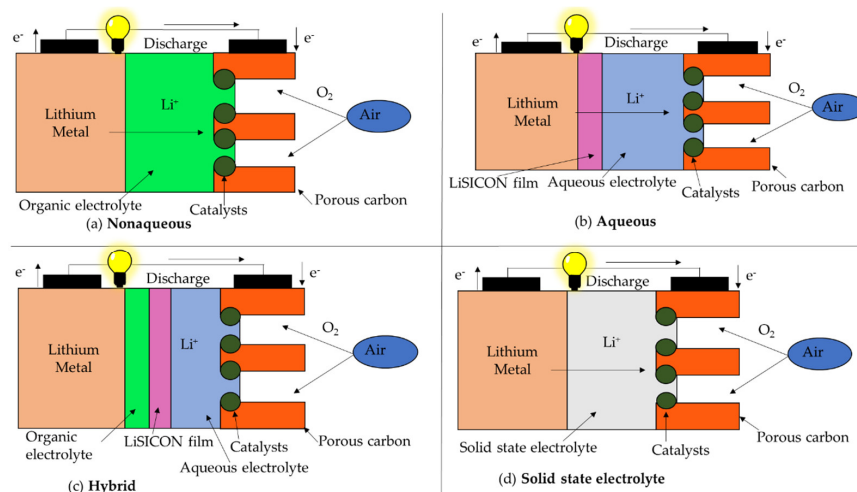

Figure 9. Metal–Air batteries cell configuration.

Table 9. Metal–Air Batteries. Characteristics and manufacturers.

Battery	Cell Reaction	Manufacturer
Li-Air	Anode: $Li \rightleftharpoons Li^+ + 1e^-$ Cathode: $Li^+ + 1e^- + O_2 \rightleftharpoons LiO_2$	American Chemical Society (Washington, DC., USA)
Zn-Air	Anode: $Zn + 4OH^- \rightleftharpoons Zn(OH)_4{}^{2-} + 2e^-$ Cathode: $1/2 O_2 + H_2O + 2e^- \rightleftharpoons 2OH^-$	NantEnergy (Scottsdale, USA), Cegasa (Vitoria, Spain), ReVolt (USA), Energizer (Saint Louis, USA).

2.4.2. Technical Comparison

The main characteristics of these batteries are good thermal stability in the range of 30–105 °C, high specific energy of 250–300 Wh/kg and 75% efficiency [62], as well as low pollution level (so they can be considered an environmentally friendly option) [61,63] and low cost, as a consequence of the abundance of raw materials [63]. However, the main drawback of these batteries is their reduced lifetime [1000 cycles] due to the precipitation of carbonate inside the electrode pores in the electrode open to the air [62].

Although these batteries are receiving more attention recently, their origin dates back to more than twenty years ago, when Abraham et al. in 1996 [64] first presented a rechargeable Li-air battery. Nevertheless, due to the rising costs of lithium and its relative scarcity compared to other materials, various scientists have been working with other materials. Then, Iudice et al. [65] propose aluminium/air batteries in seawater, with the advantage that these batteries are more stable against corrosion.

Although these batteries have high potential, they have not fulfilled it, because this technology presents challenges with the metal anode, the air cathode, the electrolyte and its short lifetime. Therefore, before this technology becomes a real option in electric vehicles or electrochemical energy storage, it is a challenge to achieve, through research and development, a specific energy of 500 Wh/kg and a lifetime of more than 1000 cycles [66].

Some commercial examples of metal-air batteries are shown in Table A4 in Appendix A.4.

Table 10 shows a summary of a technical comparison between the different battery technologies analysed in the paper.

Table 10. Summary of the technical parameters of the batteries studied in the paper.

Comparison of Battery Storage Technologies				
Characteristics	Conventional Batteries	Molten Salt Batteries	RFBs	Metal-Air Batteries
Efficiency (%)	60–97	70.7–90	60–90	75
Life cycles	500–10,000	2500–4000	2000–18,000	<1000
Specific energy (Wh/kg)	30–200	100–240	10–50	250–300

3. Hydrogen Storage. The Power of an Invisible Fuel

Hydrogen as an energy carrier was first discovered in 1789, although it was not recognised until more than a decade later [67]. In 1888, it began to be produced for commercial use, which meant that it would have to be stored somewhere.

This fuel is used as an energy carrier because of its high Lower Heating Value (LHV), 120 MJ/kg, one of the highest compared to other fossil fuels, but by contrast, the main drawback is its low volumetric density, 0.0899 g/L at ambient pressure and temperature. So this makes hydrogen storage not a minor problem [68].

On the other hand, the 2020 targets set by the EU [69] for hydrogen storage are: volumetric density—30 g/L and gravimetric density—5.3 wt. %, while the targets set for 2024 are 33 g/L volumetric density and 5.7 wt. % gravimetric density, and the targets set for 2030 are 35 g/L volumetric density and 6 wt. % gravimetric density. In the same sense, the U.S. Department of Energy (The latest DOE update date is 2020. There are no DOE targets sets for 2030) (DOE) targets are slightly more restrictive in terms of volumetric density (39 g/L) and slightly less restrictive in terms of gravimetric density (3 wt. %) [70].

Based on above, different ways of hydrogen storage have been developed. The most common techniques are summarized in Figure 10. As can be seen, techniques such as

compressed hydrogen storage or liquid hydrogen storage store pure hydrogen by increasing the pressure or decreasing the temperature, respectively. In contrast, techniques in which both pressure and temperature are kept close to ambient conditions, the hydrogen is stored mixed with other materials such as metals.
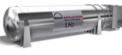
Storage technique		Volumetric H_2 density (g/L)	Gravimetric H_2 density (% wt.)	Pressure	Operation temperature
Compressed hydrogen storage		$\leq 30 \frac{g}{L}$	$\leq 6\%$	≤ 700 bar	298 K
Liquid hydrogen storage		$71 \frac{g}{L}$	100%	1 bar	21.2 K
Metal hydrides storage		$100 \frac{g}{L}$	3%	2 bar: desorption < 30 bar: adsorption	373 K (desorption)

Figure 10. Portfolio of hydrogen storage techniques.

3.1. Compressed Hydrogen Storage

Compressed hydrogen storage is currently the most common method of hydrogen storage. Typically, hydrogen gas is pressurized in a metal-composite tank at a given pressure, which can vary widely depending on the tank and its use, from 200 bar to 700 bar [71]. Higher pressures have been used for the storage of gaseous hydrogen in order to achieve volumetric densities close to that of liquid hydrogen, 70.8 g/L (about 1000 times the volumetric density of hydrogen gas at ambient pressure and temperature).

The use of the compressed hydrogen storage technique is not new. In Teeside, England, 5 MPa compressed hydrogen was stored in caverns and, in France, between 1956–1972, an aquifer was used to store a synthetic gas of 50–60% hydrogen [72]. However, as subway hydrogen storage systems were too limited to be implemented on a large scale [73], coupled with a growing interest in hydrogen in the 1970s as a result of the oil crisis [74], led to the research and development of hydrogen storage tanks, whose vessels were initially made of aluminium; however, as they were not strong enough, vessel materials were changed to a carbon-fibre composite [75].

3.1.1. Fundamental Principles

Currently, there are different types of compressed hydrogen tanks: type I are all-metal tanks in which hydrogen is usually stored between 200 and 300 bar (this type of tank has a low gravimetric density of about 1 wt. % due to the materials from which it is made); type II are metal tanks with their cylindrical part reinforced by Carbon Fibre Reinforced Polymer (CFRP) composite material, which allows this kind of tank to reach a slightly higher storage capacity than type I tanks (both type I and type II tanks are used in stationary applications); type III are tanks that have a fully CFRP-wrapped metal liner; type IV tanks are similar to type III tanks except that their liner is polymeric and not metallic (type IV tanks have reached a gravimetric density of 4.2 wt. %, because these tanks are made of lighter materials, and a volumetric density of 24 g/L at 700 bar); and, finally, type V tanks are in the development phase and are completely made of composite materials (unlined structures). Among these tanks, the most common and widely used are type III and type IV tanks due to their light weight and fatigue resistance, as well as the fact that their nominal working pressure is usually 350 to 700 bar (considerably higher than type I and type II tanks), which explains the use of these type of tanks in the automotive sector or for industrial purposes [76–78]. In addition, the industry has set a target of storing compressed hydrogen in 700 bar tanks, whereby a 6 wt. % gravimetric density and a 30 g/L volumetric density can be achieved [79]; in comparison, a 350 bar hydrogen tank has a gravimetric density of 5.5 wt. % and a volumetric density of 17.6 g/L [80]. Furthermore, this technique

has the advantage that it can be used to repeatedly (and frequently) charge and discharge the hydrogen in the tank up to a lifetime of 20 years [81]. In fact, in the case of type III tanks, they can be charged and discharged up to 5122 times before their lifetime comes to an end [82]. Although this technique consumes 2.21 kWh/kg for an isothermal compression from 0.1 to 80 MPa, this value is much lower than that of other techniques such as hydrogen liquefaction [79].

3.1.2. Mathematical Model

To know the State of Charge (SOC) of a compressed hydrogen tank, the Noble-Abel equation of state model for real gases can first be used to calculate the tank pressure [83–85] as shown in Equation (6):

$$p = \frac{\rho R T}{M_g \cdot (1 - B_{N-A}\rho)}$$

(6)

where:

M_g: molar mass of gas (g/mol)
p: gas pressure (atm)
ρ: gas density (g/L)
R: universal gas constant (0.082 (atm·L)/(K·mol))
T: gas temperature (K)
B_{N-A}: Noble-Abel constant (0.007691 L/g for hydrogen gas).

After knowing this, the SOC of the hydrogen tank will be calculated according to the expression found in Equation (7):

$$SOC(H_2\ tank) = \frac{p}{p_{max}} \cdot 100$$

(7)

where:

SOC: state of charge of the hydrogen tank (%)
p_{max}: maximum hydrogen tank pressure (atm).

This hydrogen storage technique can be used in different applications, such as small-scale storage, so it can be used in different vehicles like cars and buses [86], as a storage system in a microgrid [87] or even stored in a 700 bar tank in a hydrogen-powered snow groomer [88].

3.2. Liquid Hydrogen Storage

3.2.1. Fundamental Principles

To obtain liquid hydrogen, it is necessary to reach the hydrogen critical temperature, 33 K, i.e., almost to absolute zero. In this sense, liquid hydrogen storage tanks are at ambient pressure and a temperature of 21.2 K; in addition, the process to obtain it is a Joule-Thomson cycle in which gaseous hydrogen is first compressed, then cooled in a heat exchanger and finally expanded in a valve isenthalpically to form liquid. Although theoretically only 3.23 kWh/kg of energy are needed to liquefy hydrogen, in the practice, this values are as high as 15.2 kWh/kg, i.e., half of the Lower Heating Value (LHV) of hydrogen (33.36 kWh/kg) [89].

Although hydrogen began to be stored in liquid form in the 1940s, it was not until the 1980s and 1990s that liquid hydrogen began to be studied seriously because of its high potential [75].

This technique has the advantage of a high volumetric density, 71 g/L, compared to compressed gaseous hydrogen storage tanks [90], but the disadvantage of having to deal with boiloff ratio, which can be 0.1 to 0.2% per day of the total liquid hydrogen depending on the ratio of area to volume, so in order to reduce these losses, it is necessary to reduce the area, in proportion, more than the volume [91]. Furthermore, according to the U.S. Department of Energy (DOE), liquid hydrogen storage tanks lifetime are set at 30 years by 2025 [92].

3.2.2. Mathematical Model

To estimate liquid hydrogen storage tanks State of Charge (SOC), Equation (8) will be used to achieve this purpose:

$$SOC = \frac{m_t}{\rho_{H_2\ l} \cdot V_t} \cdot 100 \tag{8}$$

where:

SOC: state of charge of the liquid hydrogen tank (%)
m_t: hydrogen mass in the tank (g)
$\rho_{H_2\ l}$: liquid hydrogen density (71 g/L)
V_t: total volume of the liquid hydrogen storage tank (L).

Although it is currently a problem to implement liquid hydrogen storage in hydrogen-powered automotive applications, it is used in aerospace engineering [93] and in marine applications as temperature sensors [94]. One future direction for this technology is to combine with compressed hydrogen storage technology to obtain cryocompressed hydrogen storage tanks, which are capable of increasing volumetric density from 70 g/L at 1 atm to 87 g/L at 237 atm [75].

3.3. Metal Hydride Storage

3.3.1. Fundamental Principles

Metal hydrides (MHx) are the most technologically relevant class of hydrogen storage materials, as they can be used in a variety of applications at ambient pressure and temperature. In this case, gaseous hydrogen molecules are absorbed by the material in the solid state to form metallic hydrogen compounds and the hydrogen is distributed compactly throughout the metal lattice.

$$\text{Metal} + H_2 \rightleftharpoons M_xH_y + \text{Heat} \tag{9}$$
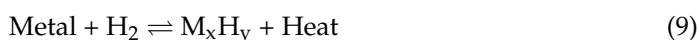
The reaction is reversible and exists as an equilibrium state under certain conditions of pressure and temperature. In other words, by changing the conditions, the reaction can move in the forward or backward direction. The heat on the right-hand side indicates that heat or energy is released when the MHx is formed (during the charging process), and therefore heat must be put into the system to release the hydrogen from the metal hydride (during the discharging process).

The origins of this technology date back to 1810, when Luigi Sementini, a professor of chemistry in Naples, published a report of a new method for extracting potassium and sodium. Many years later, Thomas Graham became interested in metal hydrides because he saw in this technology a new aspect of his studies on gas diffusion and extended the research with metals from platinum to palladium to observe the high adsorption of hydrogen. However, it was not until the laboratory work of Winkler (whose work led to the discovery of a larger number of metal hydrides), Moissan and others, that industrial developments became possible. Thus, in 1905, Bitterfeld claimed in a patent that molten calcium in an iron vessel rapidly absorbed hydrogen, and a 1943 patent established the idea of hydrogen as a fuel cell in a chemical energy package thanks to metal hydrides [95].

3.3.2. Mathematical Model

For this technology, the solid density of a fully hydrogenated metal hydride (ρ_{MH}) can be calculated thanks to the expression Equation (10) [96]:

$$\rho_{MH} = \frac{(A_{MH} + C_{MH})}{1 + \dfrac{S \cdot C_{MH}}{100 \cdot C_{MHmax}}} \cdot \frac{\rho_{MH\ initial}}{A} \tag{10}$$

where:

ρ_{MH}: hydrogenated metal hydride density (kg/m^3)

A_{MH}: fraction (molar mass H_2/molar mass unhydrated metallic alloy)
C_{MH}: atomic ratio of hydrogen to metal (H/M)
S: swelling of the alloy volume during absorption/desorption (%)
C_{MHmax}: maximum atomic ratio of hydrogen to metal (H/M)
$\rho_{MH\ initial}$: initial metal hydride density (kg/m^3).

The packing density ($\rho_{packing}$) of the metal hydride tank can be calculated by the following volumetric method applied to the material when it is not hydrogenated; for a cylindrical metal hydride tank, it will be obtained from Equation (11):

$$\rho_{packing} = \frac{m_{t\ unhyd.}}{\pi R_{MHt}^2 H} \tag{11}$$

where:

$\rho_{packing}$: metal hydride tank packing density (g/L)
$m_{t\ unhyd.}$: metal hydride tank mass when not hydrogenated (g)
$R_{MH\ t}$: metal hydride tank radius (m)
H: metal hydride tank height (m).

On the other hand, to know the charge level (SOC) in metal hydride tank, we can use Equation (12):

$$SOC = \frac{m_{MHt} - m_{t\ unhyd.}}{m_{H_2 max.}} \cdot 100 \tag{12}$$

m_{MHt}: metal hydride tank mass (g)
$m_{H_2 max}$: nominal MH tank hydrogen mass (g).

As $m_{MHT} - m_{unhyd.}$ represents the mass of hydrogen in the metal hydride tank, it can be defined as $\Delta m = m_{MHT} - m_{unhyd.}$. To estimate the evolution of the mass of hydrogen in the metal hydride tank during charging, i.e., Δm, the authors have proposed the following mathematical model Equation (13):

$$\Delta m = m_{MH\ F} \cdot \left(1 - e^{-\frac{n(t - t_0)}{t_{MH\ T}}}\right) \tag{13}$$

where:

Δm: hydrogen mass in the metal hydride tank (g)
$m_{MH\ F}$: final hydrogen mass in the metal hydride tank (g)
t: time (s)
t_0: initial time (s)
n: dimensionless constant to be adjusted by user (in case of experimental test carried by authors, $n = 5$)
$t_{MH\ T}$: total time to charge the metal hydride tank (s).

To validate this mathematical model during charging, the authors have used a (LaCe)Ni$_5$ 1500 NL metal hydride tank [97], which is externally cooled at 0.0 °C (so that the tank absorbs more hydrogen) and charged by a pressurized hydrogen tank. Thanks to a flowmeter which measures the volumetric flow in NL/h with a sample period of 1 s, it is possible to estimate the mass of hydrogen accumulated in the tank during charge process, Equation (14):

$$m_{H_2} = \sum_{i=1}^{N} \frac{\dot{V}_i \left(\frac{NL}{h}\right) \cdot \frac{1\ h}{3600\ s} \cdot \Delta t_i \cdot M_{H_2} \cdot p_N}{R \cdot T_N} \tag{14}$$

where:

m_{H_2}: hydrogen mass stored in the MH tank (g)
$\dot{V}_i$: hydrogen volumetric flow rate (NL/h)
Δt_i: time intervals (1 s)

M_{H_2}: molar mass of hydrogen (2 g/mol)
p_N: pressure at normal conditions (1 atm)
R: universal gas constant (0.082 (atm·L)/(K·mol))
T_N: temperature at normal conditions (273 K)

Once the tank is charged and $m_{MH\ F}$ and $t_{MH\ T}$ are obtained, the mathematical model can be validated by obtaining the constant n with mathematical methods (which, for this case, turns out to be 5). Figure 11 shows a comparison between measured results and the proposed mathematical model.
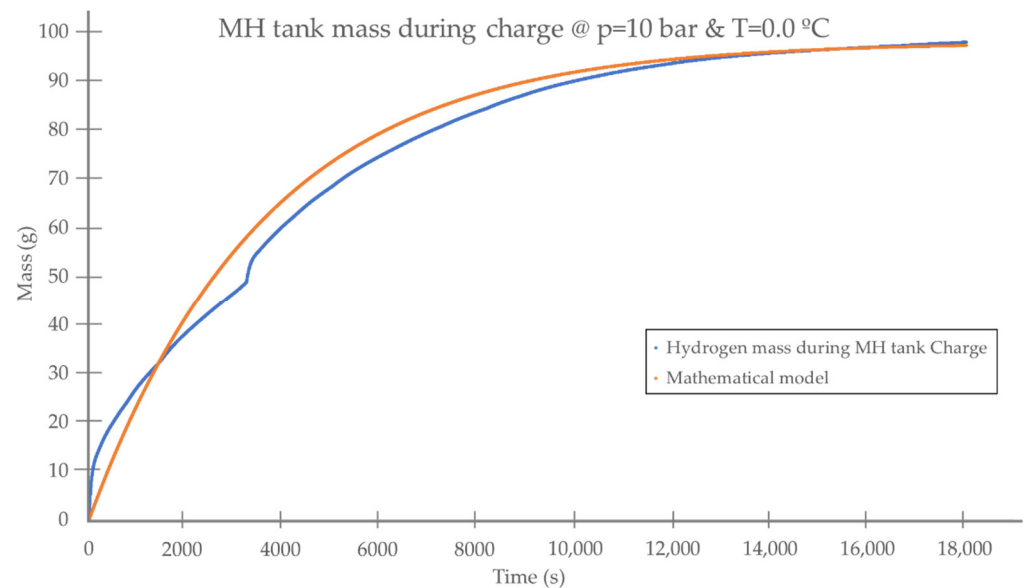

MH tank mass during charge @ p=10 bar & T=0.0 ºC

- Hydrogen mass during MH tank Charge
- Mathematical model

Figure 11. MH tank charging process. Hydrogen mass evolution.

The final charge mass of the MH tank is 97.92 g of hydrogen. To check that this is correct, the MH tank is discharged by a Polymeric Electrolyte Membrane Fuel Cell (PEM-FC) operating at a voltage of 62.13 V with an efficiency of 46.5%. The hydrogen mass discharged from the MH tank (which must be slightly less than the mass of hydrogen obtained during charging) can be calculated by Equation (15):

$$m_{H_2}(g) = \frac{\sum_{i=1}^{N} V_{FC} I_{FC-i} \Delta t_i}{LHV_{H_2} \eta_{FC}}$$

(15)

where:

m_{H_2}: hydrogen mass discharged into the MH tank (g)
V_{FC}: PEM-FC operating voltage (62.13 V)
I_{FC-i}: PEM-FC operating current for the period of time i (A)
Δt_i: period of time i (h)
LHV_{H_2}: hydrogen lower heating value (33.36 Wh/g)
η_{FC}: PEM-FC efficiency (46.5%).

Since the operating voltage of the PEM-FC is constant and its operating current is nearly constant, the discharge must be quasi-linear, as can be seen in Figure 12.
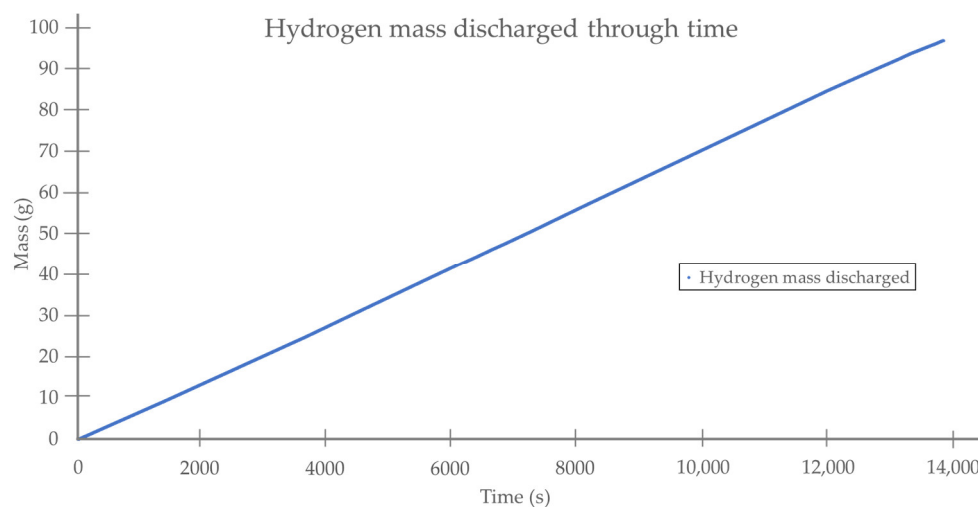
Figure 12. Hydrogen mass discharged through time.

The hydrogen mass discharged during MH tank desorption is 96.89 g, slightly lower than the hydrogen mass absorbed by the tank during the charging process. That is, the energy round-trip efficiency of MH tank reaches 98.94%.

3.3.3. Technical Comparison

Current metal hydride tanks can reach an operating charge pressure of more than 100 bar. However, for practical and economic reasons, less than 30 bar is preferred; on the other hand, the discharge process must be carried out at a pressure of about 2 bar and at a temperature below 100 °C. Although this technology provides a high volumetric density, 100 g H_2/L, its maximum gravimetric density is below 7 wt. %, but in practice, it is usually around 3 wt. %. Although this storage method has efficiency of 88% [86], its main disadvantage is the lifetime (up to 1500 cycles or 10 years) [98].

The storage materials to be combined with hydrogen in this technology include Ni, Co, Al, Mn, Sn, Cr, Fe, V, Mg, among others [86,99]. This technology can be found to be used in different applications such as stationary and mobile, heat storage, automotive, railroads or a high pressure metal hydride tank (>875 bar) for refuelling fuel cell vehicles [99,100].

3.4. Physisorption

The physisorption of gas molecules, Figure 13, onto the surface of a solid, is the result of resonant fluctuations of charge distributions (i.e., Van der Waals interactions, composed of two terms: an attractive and a repulsive one, which decrease with distance, d, in a ratio of d^{-6} and d^{-12}, respectively). For this reason, physisorption is weak, and significant physisorption can only be observed at low temperatures (<273 K) [89]. Porous materials are a potentially promising storage technology for absorbing hydrogen, since they can reach a high capacity and can release the gas reversibly [79,101]. Among all porous materials, porous carbon materials and Metal Organic Frameworks (MOFs) are known to be promising. This technology has advantages such as low cost of materials, high surface area, faster charging and discharging processes or the possibility of mitigating thermal management issues. However, the need for low pressure and temperature, the weight of carrier materials and low gravimetric and volumetric density make the application of this technology difficult. These disadvantages have meant that experiments with this technology have been unsatisfactory; and it is far from be widely used, being only possible to find applications in small-scale experiments [101].
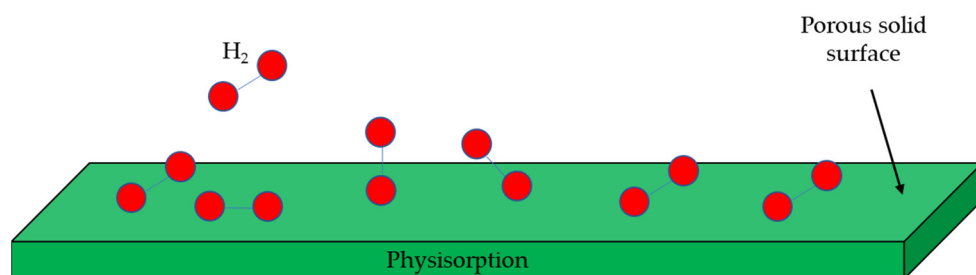
Figure 13. Physisorption process.

3.5. Complex Hydrides Storage

Complex hydrides are generally solid ions composed of cations bonded to complex anion groups (centered on Al, B or N, among others), such as AlH_4^-, NH^{2-} or NH_2^-, through a covalent bond, in which hydrogen participates. Due to slow kinetics reactions, decomposition of complex metal hydrides take place at high temperatures (in the case of $LiBH_4$, it takes place at 500 °C), while hydriding reaction take place at high pressures (up to 200 MPa) because of a faster reaction rate [102]. Figure 14 shows physical process of complex hydrides.

Although complex hydrides are known since 19th century (there is a report [103] on metal amides from 1809), it was not until the 1960s when they were started to be studied as potential hydrogen storage materials [103]. Many years later [104], in the mid-nineties, Bogdanovic discovered hydrogen uptake and release for sodium alanate, $NaAlH_4$, at moderate conditions. Later, in 2002 [104], P. Chen discovered reversible nitrogen-based complex hydrides and, in 2003, A. Züttel, and co-workers were the first to start investigating tetrahydridoboranates, such as $LiBH_4$, [104].

Complex metal   + H_2 ⟷   Complex metal hydride
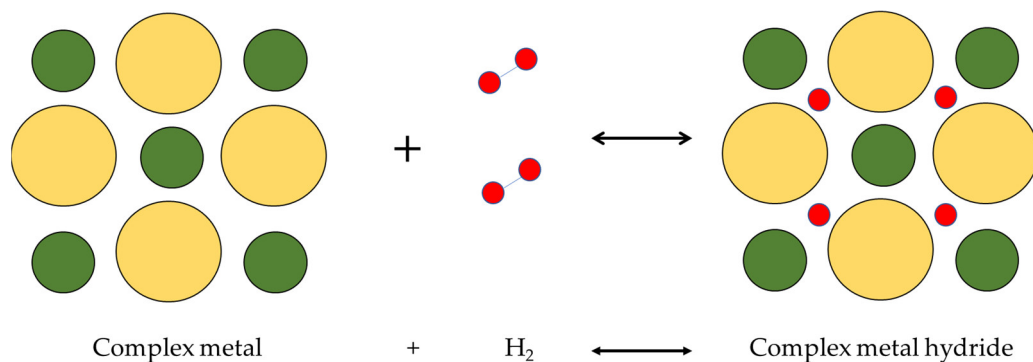
Figure 14. Complex hydrides process.

For this technology, high volumetric and gravimetric densities can be found (which will be different based on the material used). For example, for ammonia borane, NH_3BH_3, a 19.6 wt. % and a 150 g/L gravimetric and volumetric densities, respectively, are found [105], while for Mg_2FeH_6, a 5.5 wt. % and a 150 g/L gravimetric and volumetric densities, respectively, are found [106]. Furthermore, this technology has a long lifetime, with more than 5000 adsorption/desorption cycles [104]. Although these densities made complex hydrides storage a serious option to store large amounts of hydrogen (up to 700 kg [104]), this technology has to cope with issues such as thermal management (heat removal at several hundred of degrees) during refuelling [105].

This technology can be used in different applications such as on-board hydrogen storage, stationary storage, or portable power [102].

3.6. Alkalimetal + H_2O

This technology combines a particular case in complex hydrides (which it is made, for this hydrogen storage technique, from alkali or alkaline earth cations bonded to the

complex anions introduced above) with water to cause a simple reaction in which hydrogen is obtained as a product [107]. Figure 15 shows the physical process of this technology.
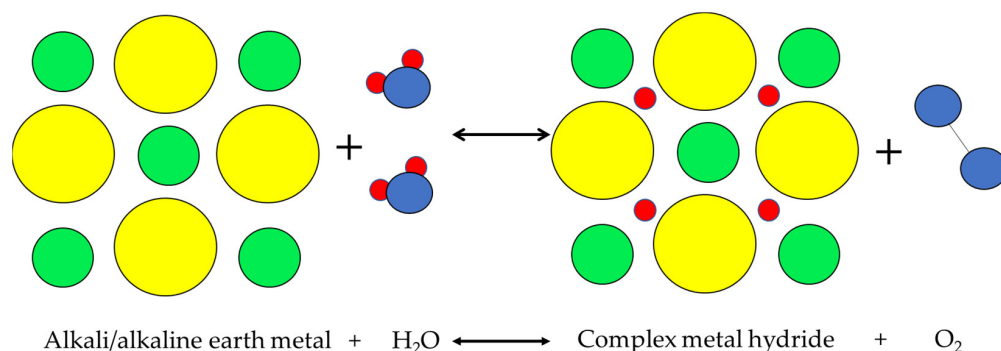

Alkali/alkaline earth metal + H_2O ⟷ Complex metal hydride + O_2

Figure 15. Alkalimetal+H_2O physical process.

This technology is far from be implemented, as it is still in the development phase. It was in 2003 that Li et al. generated hydrogen from a reaction between sodium borohydride ($NaBH_4$), with a gravimetric density of 10.6 wt. %, and water at an operating temperature of 60 °C [108].

The materials that can be used for this technique have a wide range for both volumetric and gravimetric densities, varying from 25.86 g/L for CsH to 138.08 g/L for BeH_2 in the case of volumetric density, and from 0.75 wt. % for CsH to 18.39 wt. % for $LiBH_4$ in the case of gravimetric density [107]. Furthermore, an advantage of this technology over complex hydrides is a lower operating temperature, for example, the decomposition temperature of $NaBH_4$ to obtain hydrogen is 565 °C [107], while for the reaction of this material with water, the operating temperature is just 60 °C [108]. Due to their higher gravimetric and volumetric densities, together with a higher stability of borohydrides, some of the most promising materials in this technology (still under research), $LiBH_4$, $NaBH_4$ or $Ca(BH_4)_2$, among others [107], can be found.

Once the different hydrogen storage techniques have been analysed, a comparison has been made between gravimetric and volumetric densities for the different hydrogen storage alternatives, Figure 16 (where alkali metals are treated as a particular case of complex hydrides, but in the case of a reaction with water, the operating temperature is much lower). In addition, Table 11 gives a technical comparison between the different commercial hydrogen storage technologies discussed in the paper.
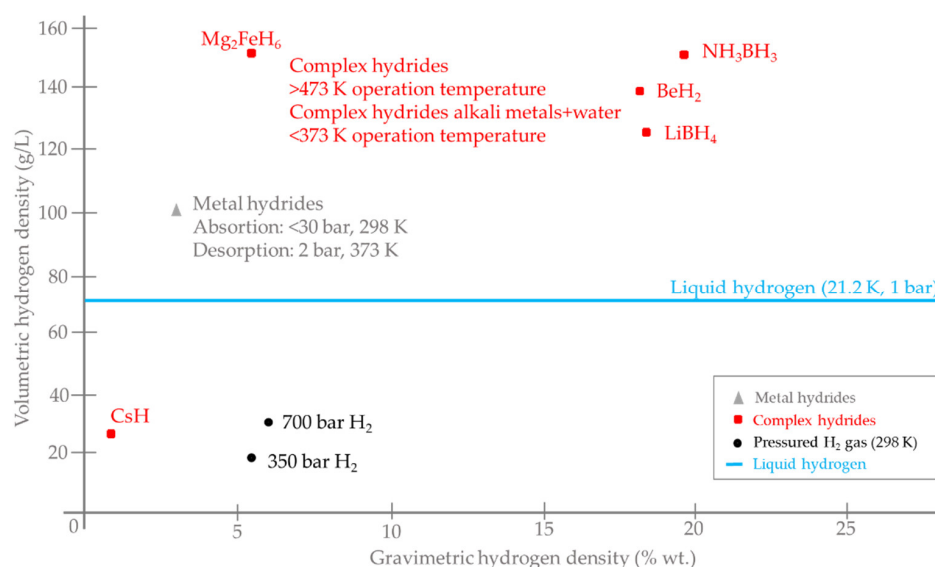

Figure 16. Alternatives for hydrogen storage: technical comparative.

Table 11. Summary of technical parameters of commercial hydrogen storage technologies.

Technology	Lifetime	Efficiency	Volumetric Density
Compressed hydrogen storage	20 years	90–95%	30 g/L
Liquid hydrogen storage	30 years (2025 DOE target)	75–80%	70.8 g/L
Metal hydrides storage	10 years	85–90%	100 g/L
Complex hydrides storage	30 years	-	150 g/L

Table A5 in Appendix B shows commercial examples for hydrogen storage solutions.

4. Batteries vs Hydrogen Storage. Substitutes or Complementary

According to the comprehensive analysis developed along the paper, there are two major green energy storage alternatives that people are considering for small and medium-sized applications: batteries and hydrogen storage. It is obvious that batteries are the most widespread (computers, mobile phones, vehicles), while hydrogen storage is used in lesser-known applications like heavy transport (trucks, buses, railways, submarines or spy-planes), or renewable sources-based microgrids.

In order to select the best choice, the first comparison to be made is the lifetime of the storage systems. For example, for a hydrogen storage system, a lifetime of 5122 cycles can be found for a type III compressed hydrogen tank [82], which is a longer lifetime than most of the batteries (only redox flow batteries and some lithium-ion batteries can present better behaviour in terms of lifetime), while for a metal hydride tank, the lifetime is up to 1500 cycles [98], which is only competitive against some battery technologies such as metal-air batteries or lead-acid batteries. On the other hand, regarding storage systems round trip efficiency, for metal hydride tanks, efficiencies of 88% can be found [86]. Although some batteries can be found with higher round-trip efficiency, this storage system is competitive against battery ones. However, contrary to battery storage systems (which convert electrical energy into chemical energy to store energy in the charging process and, in the discharging process, batteries convert chemical energy into electrical energy), a hydrogen storage system does not convert the electrical energy into chemical energy in the charging process by itself (as well as it does not convert chemical energy into electrical energy in the discharging process), since a device is needed to produce hydrogen from electrical energy. If green hydrogen (the one obtained via renewable powered electrolysis) is required to be produced, it is necessary to use an electrolyser to produce hydrogen. For an alkaline electrolyser (the most developed electrolysis technology) this process has efficiencies between 43–66% [109]. Furthermore, once the hydrogen is stored in the tank, to obtain electrical energy from it, another device is needed; if that device is a polymeric electrolyte membrane fuel cell (such as the one used to discharge the metal hydride tank in the article), with efficiency of around 46.5%. In this sense, for the whole process (production, storage and conversion into electricity), even if the energy losses associated with storage process (which in the case of metal hydride tanks, are about 12% of the stored energy), the overall efficiency is 20–31%, while for battery storage systems, the round-trip efficiency varies from 60% to 95%, i.e., between 2 and 4.75 times the hydrogen process efficiency (even if the losses associated with storage process are ignored). In addition, since the fuel cell efficiency is 46.5% (i.e., much lower than the whole round-trip efficiency of battery storage systems), the equivalent energy in a hydrogen storage tank needs to be considerably higher than the energy stored in a battery in order to obtain the same electrical energy.

Finally, although hydrogen systems (i.e., apart from the hydrogen storage, an electrolyser to produce hydrogen and a fuel cell to convert chemical energy from hydrogen into electric energy are needed) hardly can compete with batteries in terms of overall efficiency, in terms of specific energy density, hydrogen has no rival. Hydrogen has a lower heating value of 33.36 kWh/kg, i.e., more than a hundred times batteries specific energy. Therefore, hydrogen storage systems can complement batteries and be used in renewable sources-based plants as a long-term storage system, while batteries would act as short and medium-term storage system.

5. Conclusions

In this paper, two energy storage techniques have been analysed: battery and hydrogen storage systems. The main result obtained is that, in spite of the fact that batteries have been too much more useful due to the infrastructure, maybe this does not continue to be the case. As for hydrogen as an energy carrier, technology is waiting for the infrastructure to develop. It is very likely that hydrogen will take the place of fossil fuels in both the building and transportation sectors. In addition to the comprehensive study describing the fundamental principles of each technology, the authors have presented a mathematical model for both battery and hydrogen technologies. In the battery case, the model has been parametrized so that it can be used for different types of batteries. Regarding hydrogen storage, a model is proposed for each commercial hydrogen storage solution: compressed hydrogen storage, liquid hydrogen storage and metal hydride storage. Experimental tests have allowed to show the hydrogen mass evolution during the charge-discharge cycle of a 1500 NL MH tank [97], validating the corresponding proposed mathematical model. The hydrogen mass saved in the MH tank during the charging process is likely the hydrogen extracted during discharge (97.92 g vs. 96.89 g, respectively) demonstrating the high round-trip efficiency in metal hydrides.

In the future, hydrogen energy and batteries are more likely to specialize in two completely different uses—for example, batteries are practical for small devices such as mobile phones and light transport, while hydrogen storage is suitable for stationary applications and heavy transport.

Furthermore, the increase in global energy demand, along with the need to reduce dependence of fossil fuel, makes the integration of RES unavoidable. However, these systems are not always available (for example, solar energy is not available at night, or wind energy is not available when it is not windy). In that sense, ESS can be a solution to integrate RES, to improve power system security (because in case of failure of the main power grid supply, they can guarantee the load energy demand), or as a way to guarantee auxiliary services (such as battery banks in hospitals). Moreover, the different ESS reduce the need of additional resources for transmission. They also improve system efficiency, due to that they allow the system to guarantee the load energy demand when RES are not available, and a better use of existing resources due to a more controlled security and supply and production. Lastly, these systems can reduce the investment costs required for new installations.

The goal of this paper has been to analyse from a technical point of view, two different methods of energy storage—batteries and hydrogen storage systems– to try to paint a clearer picture of these methods to aid the decision to use them in real life applications. Commercial examples and technical comparisons as well as research trends and future possibilities have been detailed in an attempt to aid planning and policy decisions.

Author Contributions: Conceptualization, J.R. and F.S.; methodology, F.S. and J.R.; software, F.J.V.; validation, F.J.V.; formal analysis, J.R. and F.S.; investigation, J.R. and F.J.V.; resources, J.M.A.; data curation, F.J.V.; writing—original draft preparation, J.M.A., F.S. and J.R; writing—review and editing, J.R. and F.S.; visualization, F.J.V.; supervision, F.S. and J.M.A.; project administration, J.M.A.; funding acquisition, J.M.A. All authors have read and agreed to the published version of the manuscript.

Institutional Review Board Statement: Not applicable.

Informed Consent Statement: Not applicable.

Data Availability Statement: Not applicable.

Conflicts of Interest: The authors declare no conflict of interest.

Nomenclature

CAES	Compressed Air Energy Storage
CFRP	Carbon Fibre Reinforced Polymer
DOD	Depth Of Discharge
DOE	Department Of Energy
ESS	Energy Storage Systems
IEM	Ion-Exchange Membrane
LHV	Lower Heating Value
MHx	Metal Hydride
O&M	Operation and Maintenance
PEM-FC	Polymeric Electrolyte Membrane-Fuel Cell
RES	Renewable Energy Sources
RFB	Redox Flow Battery
SMES	Superconducting Magnetic Energy Storage
SOC	State Of Charge
ZEBRA	Zero Emission Battery Research Activity

List of Symbols

Δm	hydrogen mass in the MH tank during charge (g)
Δt_i	time intervals (1 s)
A	exponential zone amplitude (V)
A_{MH}	fraction (*molar mass H_2/molar mass unhydrated metallic alloy*)
B	inverse of the charge at the end of the exponential zone $(Ah)^{-1}$
B_{N-A}	Noble-Abel constant (0.007691 L/g for hydrogen gas)
C_{MH}	atomic ratio of hydrogen to metal (H/M)
C_{MHmax}	maximum atomic ratio of hydrogen to metal (H/M)
h	metal hydride tank height (m)
i	battery current (A)
$\int idt$	actual battery charge (Ah)
I_{FC-i}	PEM-FC operating current for a period of time (A)
K	polarization voltage (V)
LHV_{H_2}	hydrogen lower heating value (33.36 Wh/g)
M_g	molar mass of gas (g/mol)
M_{H_2}	molar mass of hydrogen (2 g/mol)
$m_{H_2}\,(g)$	hydrogen mass charged (or discharged) into the MH tank
m_{H_2max}	nominal MH tank hydrogen mass (g)
$m_{MH\,F}$	final hydrogen mass in the MH tank (g)
m_{MHt}	metal hydride tank mass (g)
m_t	hydrogen mass in the tank (g)
$m_{t\,unhyd.}$	metal hydride tank mass when not hydrogenated (g)
η_{FC}	yield of the PEM-FC (46.5%)
n	dimensionless constant to be adjusted by user (in case of experimental test arried 5 by authors, $n = 5$)
ρ	gas density (g/L)
$\rho_{H_2\,l}$	liquid hydrogen density (71 g/L)
ρ_{MH}	hydrogenated metal hydride density (g/L)
$\rho_{MH\,initial}$	initial metal hydride density (g/L)
$\rho_{packing}$	metal hydride tank packing density (g/L)
p	gas pressure (atm)
p_{max}	maximum hydrogen tank pressure (atm)
p_N	pressure at normal conditions (1 atm)
Q	battery capacity (Ah)
Q_{exp}	battery capacity at the end of exponential zone (Ah)
Q_{NOM}	battery capacity at the end of nominal zone (Ah)
R	universal gas constant (0.082 (atm·L)/(K·mol))
R_{elec}	internal resistance (Ω)
$R_{MH\,t}$	metal hydride tank radius (m)
S	swelling of the alloy volume during absorption/desorption (%)

SOC	state of charge (%)
t	time (s)
T	gas temperature (K)
$T_{MH\ T}$	total time to charge a MH tank (s)
T_N	temperature at normal conditions (273 K)
t_0	initial time (s)
V	no load voltage (V)
V_0	battery constant voltage (V)
V_b	battery voltage (V)
V_{exp}	voltage at end of exponential zone (V)
V_{FC}	PEM-FC operating voltage (62.13 V)
V_{full}	fully charged battery voltage (V)
$\dot{V}_i \left(\frac{NL}{h} \right)$	hydrogen volumetric flow rate
V_{NOM}	voltage at the end of nominal zone (V)
V_t	total volume of the hydrogen tank (L)

Appendix A. Battery Technology

Appendix A.1. Conventional Technology

The batteries included in this group are the most common and the most extended in the market, like Lead-Acid, Nickel-Cadmium and Lithium-ion batteries. All of them have in common a redox reaction in which one of the electrodes releases ions and the electrolyte carries them to the other side.

Table A1. Commercial examples of conventional batteries. Data provided by the manufacturer.
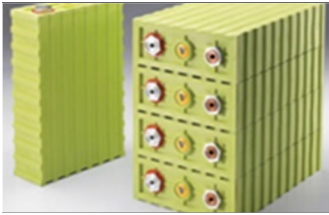
Lead-Acid	
	Model: 6GFMJ-65 Battery capacity: 65 Ah/12 V Lifetime: $\geq$10 years Dimensions: X-350 mm, Y-166 mm, Z-174 mm Weight: 21.4 kg Cost: 57 *d*
	Model: EP200-12 Battery capacity: 200 Ah/12 V Lifetime: 3–5 years Dimensions: X-533 mm, Y-250 mm, Z-240 mm Weight: 62.95 kg Cost: 201.87 *d* (1 ₹ = 0.012 *d* (3 August 2022))

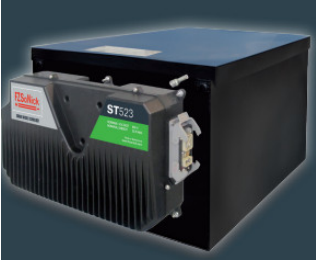| Nickel-Cadmium	
	Model: N-3000CR Battery capacity: 3000 mAh/1.2 V Lifetime: 1 cycle Dimensions: Diameter-26 mm, Height-50 mm Weight: 86 g Cost: 6.86 *d*
	Model: VNT D U HC Battery capacity: 4500 mAh/1.2 V Lifetime: $\geq$4 years (55 °C) Dimensions: Diameter-32.15 mm, Height-59.9 mm Weight: 124 g Cost: 25.40 *d* (1 £ = 1.20 *d* (3 August 2022))

Table A1. *Cont.*

Lithium-ion

Model V-LYP400Ah 3.2 V
Stored energy: 1.2 kWh
Lifetime: 2000 cycles
Dimensions: X-460 mm, Y-285 mm, Z-65 mm
Weight: 13.5 kg
Cost: 550 *d*

Model: LG Chem RESU10H
Energy stored: 9.8 kWh
Battery capacity: 189 Ah
Lifetime: ≥10 years
Dimensions: X-452.12 mm, Y-482.6 mm, Z-226.06 mm
Weight: 74.9 kg
Cost: 5996.3 *d* (1 $ = 1.01 *d* (3 August 2022))

Appendix A.2. Molten Salt Technology

The batteries included in this group are characterized by their high operating temperature and high specific energy. Both ZEBRA and NAS batteries have in common a cylindrical cell structure where molten salts and alumina are used for electrode and electrolyte respectively.
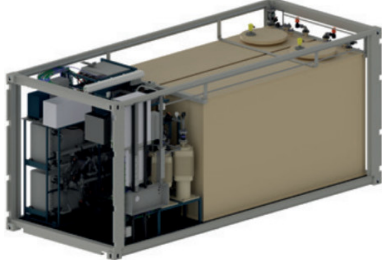
Table A2. Commercial examples of Molten Salt batteries. Data provided by the manufacturer.

ZEBRA

Model ZEBRA Z5278-ML3X-64
Stored energy: 17.8 kWh
Lifetime: 3500 cycles
Dimensions: X-826 mm, Y-530 mm, Z-295 mm
Weight: 182 Kg
Cost: 1500 *d*

Model: FZSonick ST523
Battery capacity: 38 Ah/620 V
Stored energy: 22.5 kWh
Lifetime: >4500 cycles (80% DOD)
Dimensions: X-624 mm, Y-406 mm, Z-1023 mm
Weight: 256 kg
Cost-18,000 *d*

NAS

Model: BASF NAS® Battery
Stored energy: 1450 kWh
Lifetime: 20 years; 4000 cycles
Dimensions: X-6058 mm, Y-2438 mm, Z-2591 mm
Weight: 21 tons
Cost: Non available

Appendix A.3. Redox Flow Technology

This type of battery is characterized by the fact that the electrolyte is stored in a tank that is separated from the own cell structure. Additionally, there is no material transfer between electrode and electrolyte, so the lifetime is independent of DOD.
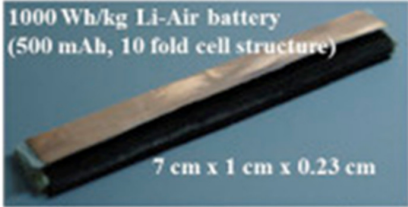
Table A3. Commercial examples of Redox Flow Batteries. Data provided by the manufacturer.

ICB	
	Model Enervalut Proyect Nominal power: 250 kW Lifetime: research Weight: tonnes Cost: Investment 4672,900 *d*
ZnBr	
	Model: ZBM2 Stored energy: 10 kWh Lifetime: 10 years Dimensions: X-830 mm, Y-823 mm, Z-400 mm Weight: 240 kg Cost: 7921 *d* (1 \$ = 1.01 *d* (3 August 2022))
	Model: ZBM3 Stored energy: 10 kWh Lifetime: 10 years Dimensions: X-861 mm, Y-747 mm, Z-400 mm Weight: 240 kg Cost: 8713 *d* (1 \$ = 1.01 *d* (3 August 2022))
VRB	
	Model: RFB40X P1. Nominal power: 40 kW Stored energy: 40 kWh Lifetime: >20 years Dimensions: X-2300 mm, Y-1400 mm, Z-1900 mm Weight: 3400 kg Cost: 44,780.6 *d* (1 ₹ = 0.012 *d* (3 August 2022))
	Model: E22 VRB Battery. Nominal power: 50 kW Stored energy: 200 kWh Lifetime: >10,000 cycles; >20 years Dimensions: X-6000 mm, Y-2400 mm, Z-2600 mm Weight: 24,000 kg Cost: Non available

Appendix A.4. Metal-Air Technology

This type of battery is characterized by an open cathode structure, where air enters and, in the presence of a catalyst, oxygen reacts with the metal-ions. This allows to increase the specific energy with respect to conventional rechargeable batteries.

Table A4. Commercial examples of Metal-Air Batteries. Data provided by the manufacturer.

Li-Air	
	Model Li -Air 500 mAh Samsung Electronics Battery capacity: 500 mAh Lifetime: 7 cycles Dimensions: X-70 mm, Y-10 mm, Z-23 mm Weight: 35 mg Cost: Non available
Zn-Air	
	Model DQFC 24/24-125 Stored energy: 2.88 kWh Lifetime: 300 cycles Dimensions: X-410 mm, Y-220 mm, Z-240 mm Weight: 21.8 kg Cost: 300 *d*

Appendix B. Hydrogen Storage

In this Appendix, authors show commercial examples of hydrogen storage devices. Nowadays, it is possible to find two commercial options for hydrogen storage: compressed hydrogen storage and metal hydride storage.

Table A5. Commercial examples of Hydrogen storage. Data provided by the manufacturer.

Compressed Gas Hydrogen Storage	
	Model B50 Stored energy: 26.7 kWh Vol. H_2: 8900 NL Vol. bottle: 50 L Pressure: 200 bar Dimensions: H-1680 mm, Ø-230 mm Weight: 85 kg Cost: 200 *d* annual contract
Metal Hydride storage	
	Model Hbond 5000 L Stored energy: 15 kWh Vol. H_2: 5000 NL Vol. bottle: 98.6 L Pressure: 15 bar Dimensions: H-1100 mm, Ø-169 mm Weight: 76 kg Cost: 10,000 *d*

References

1. Russo, M.A.; Carvalho, D.; Martins, N.; Monteiro, A. Forecasting the inevitable: A review on the impacts of climate change on renewable energy resources. *Sustain. Energy Technol. Assess.* **2022**, *52*, 102283. [CrossRef]
2. Zhang, Z.; Ding, T.; Zhou, Q.; Sun, Y.; Qu, M.; Zeng, Z.; Ju, Y.; Li, L.; Wang, K.; Chi, F. A review of technologies and applications on versatile energy storage systems. *Renew. Sustain. Energy Rev.* **2021**, *148*, 111263. [CrossRef]
3. Communication, L.S. The smart grid: An introduction. *Smart Grid Electr. Power Transm.* **2011**, 1–45. [CrossRef]
4. Walker, T.J. EPRI Intelligrid/Smart Grid Demonstration Joint Advisory Meeting. *System* **2010**, 1–16.
5. Eustis, C.; Gyuk, I. Energy Storage Safety Strategic Plan Acknowledgements. 2014. Available online: https://vdocuments.net/energy-storage-safety-strategic-safety-strategic-planenergy-storage-safety-strategic.html?page=1 (accessed on 25 July 2022).
6. AL Shaqsi, A.Z.; Sopian, K.; Al-Hinai, A. Review of energy storage services, applications, limitations, and benefits. *Energy Rep.* **2020**, *6*, 288–306. [CrossRef]
7. Pershaanaa, M.; Bashir, S.; Ramesh, S.; Ramesh, K. Every bite of Supercap: A brief review on construction and enhancement of supercapacitor. *J. Energy Storage* **2022**, *50*, 104599. [CrossRef]
8. Fiore, M.; Magi, V.; Viggiano, A. Internal combustion engines powered by syngas: A review. *Appl. Energy* **2020**, *276*, 115415. [CrossRef]
9. Rullo, P.; Braccia, L.; Luppi, P.; Zumoffen, D.; Feroldi, D. Integration of sizing and energy management based on economic predictive control for standalone hybrid renewable energy systems. *Renew. Energy* **2019**, *140*, 436–451. [CrossRef]
10. Piccolino, M. The bicentennial of the Voltaic battery (1800-2000): The artificial electric organ. *Trends Neurosci.* **2000**, *23*, 147–151. [CrossRef]
11. Kurzweil, P. Gaston Planté and his invention of the lead-acid battery-The genesis of the first practical rechargeable battery. *J. Power Sources* **2010**, *195*, 4424–4434. [CrossRef]
12. Kandeeban, R.; Saminathan, K.; Manojkumar, K.; Dilsha, C.G.; Krishnaraj, S. Battery economy: Past, present and future. *Mater. Today Proc.* **2019**, *48*, 143–147. [CrossRef]
13. Mitali, J.; Dhinakaran, S.; Mohamad, A.A. Energy storage systems: A review. *Energy Storage Sav.* 2022; *in press*. [CrossRef]
14. Winter, M.; Brodd, R.J. What are batteries, fuel cells, and supercapacitors? *Chem. Rev.* **2004**, *104*, 4245–4269. [CrossRef] [PubMed]
15. Ghiji, M.; Novozhilov, V.; Moinuddin, K.; Joseph, P.; Burch, I.; Suendermann, B.; Gamble, G. A Review of Lithium-Ion Battery Fire Suppression. *Energies* **2020**, *13*, 5117. [CrossRef]
16. Riaz, A.; Sarker, M.R.; Saad, M.H.M.; Mohamed, R. Review on Comparison of Different Energy Storage Technologies Used in Micro-Energy Harvesting, WSNs, Low-Cost Microelectronic Devices: Challenges and Recommendations. *Sensors* **2021**, *21*, 5041. [CrossRef]
17. Valve-Regulated Lead-Acid (VRLA) Gelled Electrolyte (gel) and Absorbed Glass Mat (AGM) Batteries. Available online: https://www.mkbattery.com/application/files/9615/3374/2592/Valve_Regulated_Lead-Acid_VRLA_Gel_and_AGM_batteries.pdf (accessed on 25 July 2022).
18. Asghar, R.; Rehman, F.; Ullah, Z.; Qamar, A.; Ullah, K.; Iqbal, K.; Aman, A.; Nawaz, A.A. Electric vehicles and key adaptation challenges and prospects in Pakistan: A comprehensive review. *J. Clean. Prod.* **2021**, *278*, 123375. [CrossRef]
19. Tucker, C. Battery Information Sheet. *FlashCAV* **2010**, *49*, 1–8.
20. Nickel—Cadmium Batteries Operating and Nickel—Cadmium Airborne Batteries. Available online: https://www.enersys.com/493bb4/globalassets/documents/product-documentation/_enersys/emea/legacy/batteries/hawker/aviation/enersys_ni-cad_aircraft_maint_manual_may-2013_version1_en.pdf (accessed on 25 July 2022).
21. Technical Manual Lomain Ni-Cd Pocket Plate Battery, n.d. Available online: https://www.gaz-gmbh.com/UserFiles/Image/1575292176GAZ-Manual-lomain-2019.pdf (accessed on 25 July 2022).
22. Liu, Y.; Zhang, R.; Wang, J.; Wang, Y. Current and future lithium-ion battery manufacturing. *iScience* **2021**, *24*, 102332. [CrossRef]
23. Ruetschi, P. Review on the lead-acid battery science and technology. *J. Power Sources* **1977**, *2*, 3–120. [CrossRef]
24. Pavlov, D. *Lead-Acid Batteries: Science and Technology: A Handbook of Lead-Acid Battery Technology and Its Influence on the Product*; Elsevier: Amsterdam, The Netherlands, 2011; p. 722.
25. Industrial Batteries 101. Available online: http://site.ieee.org/fw-pes/files/2018/07/Industrial-Batteries-101-IEEE-PES-Ft-Worth.pdf (accessed on 25 April 2022).
26. Johnson, S.C.; Todd Davidson, F.; Rhodes, J.D.; Coleman, J.L.; Bragg-Sitton, S.M.; Dufek, E.J.; Webber, M.E. Selecting Favorable Energy Storage Technologies for Nuclear Power. *Storage Hybrid. Nucl. Energy Techno-Econ. Integr. Renew. Nucl. Energy* **2019**, 119–175. [CrossRef]
27. Sarma, D.D.; Shukla, A.K. Building better batteries: A travel back in time. *ACS Energy Lett.* **2018**, *3*, 2841–2845. [CrossRef]
28. Xie, J.; Lu, Y.C. A retrospective on lithium-ion batteries. *Nat. Commun.* **2020**, *11*, 9–12. [CrossRef] [PubMed]
29. Scrosati, B. History of lithium batteries. *J. Solid State Electrochem.* **2011**, *15*, 1623–1630. [CrossRef]
30. Tremblay, O.; Dessaint, L.; Dekkiche, A. A Generic Battery Model for the Dynamic Simulation of Hybrid Electric Vehicles. In Proceedings of the IEEE Vehicle Power and Propulsion Conference, Arlington, TX, USA, 9–12 September 2007; pp. 284–289.
31. Lutgens, F.K.; Tarbuck, E.J.; Tasa, D.G. *Essentials of Geology, Global Edition*; Pearson: London, UK, 2015.
32. Scrosati, B.; Garche, J. Lithium batteries: Status, prospects and future. *J. Power Sources* **2010**, *195*, 2419–2430. [CrossRef]
33. Wang, W.; Yuan, B.; Sun, Q.; Wennersten, R. Application of energy storage in integrated energy systems—A solution to fluctuation and uncertainty of renewable energy. *J. Energy Storage* **2022**, *52*, 104812. [CrossRef]

34. Choudhury, S. Review of energy storage system technologies integration to microgrid: Types, control strategies, issues, and future prospects. *J. Energy Storage* **2022**, *48*, 103966. [CrossRef]
35. Zakeri, B.; Syri, S. Electrical energy storage systems: A comparative life cycle cost analysis. *Renew. Sustain. Energy Rev.* **2015**, *42*, 569–596. [CrossRef]
36. Liu, J.; Hu, C.; Kimber, A.; Wang, Z. Uses, Cost-Benefit Analysis, and Markets of Energy Storage Systems for Electric Grid Applications. *J. Energy Storage* **2020**, *32*, 101731. [CrossRef]
37. Elio, J.; Phelan, P.; Villalobos, R.; Milcarek, R.J. A review of energy storage technologies for demand-side management in industrial facilities. *J. Clean. Prod.* **2021**, *307*, 127322. [CrossRef]
38. Banerjee, A.; Ziv, B.; Shilina, Y.; Levi, E.; Luski, S.; Aurbach, D. Single-wall carbon nanotube doping in lead-acid batteries: A new horizon. *ACS Appl. Mater. Interfaces* **2017**, *9*, 3634–3643. [CrossRef]
39. Gangaja, B.; Nair, S.; Santhanagopalan, D. Reuse, Recycle, and Regeneration of LiFePO4Cathode from Spent Lithium-Ion Batteries for Rechargeable Lithium- and Sodium-Ion Batteries. *ACS Sustain. Chem. Eng.* **2021**, *9*, 4711–4721. [CrossRef]
40. Energy Storage Technology Descriptions-EASE-European Associaton for Storage of Energy. Available online: www.ease-storage.eu (accessed on 11 April 2022).
41. Dustmann, C.H. Advances in ZEBRA batteries. *J. Power Sources* **2004**, *127*, 85–92. [CrossRef]
42. Wen, Z.; Cao, J.; Gu, Z.; Xu, X.; Zhang, F.; Lin, Z. Research on sodium sulfur battery for energy storage. *Solid State Ion.* **2008**, *179*, 1697–1701. [CrossRef]
43. Capasso, C.; Veneri, O. Integration between Super-capacitors and ZEBRA Batteries as High Performance Hybrid Storage System for Electric Vehicles. *Energy Procedia* **2017**, *105*, 2539–2544. [CrossRef]
44. Kumar, D.; Kuhar, S.B.; Kanchan, D.K. Room temperature sodium-sulfur batteries as emerging energy source. *J. Energy Storage* **2018**, *18*, 133–148. [CrossRef]
45. Shamim, N.; Thomsen, E.C.; Viswanathan, V.V.; Reed, D.M.; Sprenkle, V.L.; Li, G. Evaluating ZEBRA Battery Module under the Peak-Shaving Duty Cycles. *Materials* **2021**, *14*, 2280. [CrossRef]
46. Aneke, M.; Wang, M. Energy storage technologies and real life applications—A state of the art review. *Appl. Energy* **2016**, *179*, 350–377. [CrossRef]
47. Chauhan, A.; Saini, R.P. A review on Integrated Renewable Energy System based power generation for stand-alone applications: Configurations, storage options, sizing methodologies and control. *Renew. Sustain. Energy Rev.* **2014**, *38*, 99–120. [CrossRef]
48. Weber, A.Z.; Mench, M.M.; Meyers, J.P.; Ross, P.N.; Gostick, J.T.; Liu, Q. Redox flow batteries: A review. *J. Appl. Electrochem.* **2011**, *41*, 1137–1164. [CrossRef]
49. Sun, C.; Negro, E.; Nale, A.; Pagot, G.; Vezzù, K.; Zawodzinski, T.A.; Meda, L.; Gambaro, C.; Di Noto, V. An efficient barrier toward vanadium crossover in redox flow batteries: The bilayer [Nafion/(WO3)x] hybrid inorganic-organic membrane. *Electrochim. Acta* **2021**, *378*, 138133. [CrossRef]
50. Xu, Z.; Fan, Q.; Li, Y.; Wang, J.; Lund, P.D. Review of zinc dendrite formation in zinc bromine redox flow battery. *Renew. Sustain. Energy Rev.* **2020**, *127*, 109838. [CrossRef]
51. Alotto, P.; Guarnieri, M.; Moro, F. Redox flow batteries for the storage of renewable energy: A review. *Renew. Sustain. Energy Rev.* **2014**, *29*, 325–335. [CrossRef]
52. Vanýsek, P.; Novák, V. Redox flow batteries as the means for energy storage. *J. Energy Storage* **2017**, *13*, 435–441. [CrossRef]
53. Clemente, A.; Costa-Castelló, R. Redox Flow Batteries: A Literature Review Oriented to Automatic Control. *Energies* **2020**, *13*, 4514. [CrossRef]
54. Rajarathnam, G.P.; Montoya, A.; Vassallo, A.M. The influence of a chloride-based supporting electrolyte on electrodeposited zinc in zinc/bromine flow batteries. *Electrochim. Acta* **2018**, *292*, 903–913. [CrossRef]
55. Jiménez-Blasco, U.; Moreno, E.; Cólera, M.; Díaz-Carrasco, P.; Arrebola, J.C.; Caballero, A.; Morales, J.; Vargas, A. Enhanced Performance of Zn/Br Flow Battery Using N-Methyl-N-Propylmorpholinium Bromide as Complexing Agent. *Int. J. Mol. Sci. Artic.* **2021**, *22*, 9288. [CrossRef]
56. Bartolozzi, M. Development of redox flow batteries. A historical bibliography. *J. Power Sources* **1989**, *27*, 219–234. [CrossRef]
57. Zeng, Y.K.; Zhou, X.L.; An, L.; Wei, L.; Zhao, T.S. A high-performance flow-field structured iron-chromium redox flow battery. *J. Power Sources* **2016**, *324*, 738–744. [CrossRef]
58. Solid Electrode Battery Technology | Energy Storage Assocation. Available online: https://energystorage.org/why-energy-storage/technologies/solid-electrode-batteries/ (accessed on 12 April 2022).
59. Prifti, H.; Parasuraman, A.; Winardi, S.; Lim, T.M.; Skyllas-Kazacos, M. Membranes for redox flow battery applications. *Membranes* **2012**, *2*, 275–306. [CrossRef]
60. Lee, J.-S.; Kim, S.T.; Cao, R.; Choi, N.-S.; Liu, M.; Lee, K.T.; Cho, J. Metal-air batteries with high energy density: Li-air versus Zn-air. *Adv. Energy Mater.* **2011**, *1*, 34–50. [CrossRef]
61. Wang, Y.; Pan, W.; Luo, S.; Zhao, X.; Kwok, H.Y.H.; Xu, X.; Leung, D.Y. High-performance solid-state metal-air batteries with an innovative dual-gel electrolyte. *Int. J. Hydrogen Energy* **2022**, *47*, 15024–15034. [CrossRef]
62. Crompton, T.R. Battery reference book—Second Edition. *Fuel Energy Abstr.* **1996**, *37*, 192. [CrossRef]
63. Li, S.; Guo, H.; He, S.; Yang, H.; Liu, K.; Duan, G.; Jiang, S. Advanced electrospun nanofibers as bifunctional electrocatalysts for flexible metal-air (O2) batteries: Opportunities and challenges. *Mater. Des.* **2022**, *214*, 110406. [CrossRef]

64. Abraham, K.M.; Jiang, Z. A Polymer Electrolyte—Based Rechargeable Lithium/Oxygen Battery TECHNICAL PAPERS ELECTRO-CHEMICAL SCIENCE AND TECHNOLOGY A Polymer Electrolyte-Based Rechargeable lithium/Oxygen Battery. *J. Electrochem. Soc.* **1996**, *143*, 1–5. [CrossRef]

65. Iudice de Souza, J.P.B.; Belem, U.F.d.P.; Vielstich, W.B. IQSC, Sao Carlos, Universidade de Sao Paulo Seawater aluminum/air cells. *Handb. Fuel Cells Fundam. Technol. Appl.* **2003**, *1*, 409–415.

66. Li, Y.; Lu, J. Metal−Air Batteries: Will They Be the Future Electrochemical Energy Storage Device of Choice? *ACS Energy Lett.* **2017**, *2*, 15. [CrossRef]

67. Paidar, M.; Fateev, V.; Bouzek, K. Membrane electrolysis–History, current status and perspective. *Electrochim. Acta* **2016**, *209*, 737–756. [CrossRef]

68. Bhasker, J.P.; Porpatham, E. Effects of compression ratio and hydrogen addition on lean combustion characteristics and emission formation in a Compressed Natural Gas fuelled spark ignition engine. *Fuel* **2017**, *208*, 260–270. [CrossRef]

69. Fuel Cells and Hydrogen 2 Joint Undertaking (FCH JU). *Addendum to the Multi-Annual Work Plan 2014–2020*; European Commission's Horizon 2020 Programme for Research and Innovation; FCH JU: Brussels, Belgium, 2018.

70. Menezes, M.W.; Simmons, D.R.; Winberg, S.; Baranwal, R.; Hoffman, P.; Genatowski, S.L. U.S. Department of Energy Hydrogen Program Plan. Available online: https://www.hydrogen.energy.gov/pdfs/hydrogen-program-plan-2020.pdf (accessed on 23 April 2022).

71. Quantum Fuel Systems Technologies, Worldwide I. High-Pressure Hydrogen Storage Systems. 2004. Available online: http://www.pnl.gov/fuelcells/docs/summits/summit8/presentations/day2/abele%7B%5C_%7D915am.pdf (accessed on 24 April 2004).

72. Lindblom, U.E. A Conceptual Design for Compressed Hydrogen Storage in Mined Caverns. *Int. J. Hydrogen Energy* **1985**, *10*, 667–675. [CrossRef]

73. Thiyagarajan, S.R.; Emadi, H.; Hussain, A.; Patange, P.; Watson, M. A comprehensive review of the mechanisms and efficiency of underground hydrogen storage. *J. Energy Storage* **2022**, *51*, 104490. [CrossRef]

74. Arsad, A.Z.; Hannan, M.A.; Al-Shetwi, A.Q.; Mansur, M.; Muttaqi, K.M.; Dong, Z.Y.; Blaabjerg, F. Hydrogen energy storage integrated hybrid renewable energy systems: A review analysis for future research directions. *Int. J. Hydrogen Energy* **2022**, *47*, 17285–17312. [CrossRef]

75. Durbin, D.J.; Malardier-Jugroot, C. Review of hydrogen storage techniques for on board vehicle applications. *Int. J. Hydrogen Energy* **2013**, *38*, 14595–14617. [CrossRef]

76. Zhao, L.; Zhao, Q.; Zhang, J.; Zhang, S.; He, G.; Zhang, M.; Su, T.; Liang, X.; Huang, C.; Yan, W. Review on studies of the emptying process of compressed hydrogen tanks. *Int. J. Hydrogen Energy* **2021**, *46*, 22554–22573. [CrossRef]

77. Landi, D.; Vita, A.; Borriello, S.; Scafà, M.; Germani, M. A Methodological Approach for the Design of Composite Tanks Produced by Filament Winding. *Comput. Des. Appl.* **2020**, *17*, 1229–1240. [CrossRef]

78. Hassan, I.A.; Ramadan, H.S.; Saleh, M.A.; Hissel, D. Hydrogen storage technologies for stationary and mobile applications: Review, analysis and perspectives. *Renew. Sustain. Energy Rev.* **2021**, *149*, 111311. [CrossRef]

79. Zhou, L. Progress and problems in hydrogen storage methods. *Renew Sustain. Energy Rev.* **2005**, *9*, 395–408. [CrossRef]

80. Technical Assessment of Compressed Hydrogen Storage Tank Systems for Automotive Applications Nuclear Engineering Division. 2010. Available online: www.anl.gov (accessed on 13 April 2022).

81. Monforti Ferrario, A.; Bartolini, A.; Segura Manzano, F.; Vivas, F.J.; Comodi, G.; McPhail, S.J.; Andujar, J.M. A model-based parametric and optimal sizing of a battery/hydrogen storage of a real hybrid microgrid supplying a residential load: Towards island operation. *Adv. Appl. Energy* **2021**, *3*, 100048. [CrossRef]

82. Zhang, M.; Lv, H.; Kang, H.; Zhou, W.; Zhang, C. A literature review of failure prediction and analysis methods for composite high-pressure hydrogen storage tanks. *Int. J. Hydrogen Energy* **2019**, *44*, 25777–25799. [CrossRef]

83. Florio, L.A. Effect of gas equation of state on CFD predictions for ignition characteristics of hydrogen escaping from a tank. *Int. J. Hydrogen Energy* **2014**, *39*, 18451–18471. [CrossRef]

84. Li, J.Q.; Myoung, N.S.; Kwon, J.T.; Jang, S.J.; Lee, T. A Study on the Prediction of the Temperature and Mass of Hydrogen Gas inside a Tank during Fast Filling Process. *Energies* **2020**, *13*, 6428. [CrossRef]

85. Le Métayer, O.; Saurel, R. The Noble-Abel Stiffened-Gas equation of state. *Phys. Fluids* **2016**, *28*, 046102. [CrossRef]

86. Ni, M. An Overview of Hydrogen Storage Technologies. *ENERGY Explor. Exploit.* **2006**, *24*, 197–209. [CrossRef]

87. Ferrario, A.M.; Vivas, F.J.; Manzano, F.S.; Andújar, J.M.; Bocci, E.; Martirano, L. Hydrogen vs. Battery in the long-term operation. A comparative between energy management strategies for hybrid renewable microgrids. *Electronics* **2020**, *9*, 698. [CrossRef]

88. Composite cylinders for hydrogen-powered snow groomer. *Reinf. Plast.* **2021**, *65*, 66. [CrossRef]

89. Züttel, A. Materials for hydrogen storage. *Mater. Today* **2003**, *6*, 24–33. [CrossRef]

90. Choi, Y.; Kim, J.; Park, S.; Park, H.; Chang, D. Design and analysis of liquid hydrogen fuel tank for heavy duty truck. *Int. J. Hydrogen Energy* **2022**, *47*, 14687–14702. [CrossRef]

91. Berstad, D.; Gardarsdottir, S.; Roussanaly, S.; Voldsund, M.; Ishimoto, Y.; Nekså, P. Liquid hydrogen as prospective energy carrier: A brief review and discussion of underlying assumptions applied in value chain analysis. *Renew. Sustain. Energy Rev.* **2022**, *154*, 111772. [CrossRef]

92. Aziz, M. Liquid hydrogen: A review on liquefaction, storage, transportation, and safety. *Energies* **2021**, *14*, 5917. [CrossRef]

93. Tang, X.; Pu, L.; Shao, X.; Lei, G.; Li, Y.; Wang, X. Dispersion behavior and safety study of liquid hydrogen leakage under different application situations. *Int. J. Hydrogen Energy* **2020**, *45*, 31278–31288. [CrossRef]

94. Nakano, A.; Shimazaki, T.; Sekiya, M.; Shiozawa, H.; Ohtsuka, K.; Aoyagi, A.; Iwakiri, T.; Mikami, Z.; Sato, M.; Sugino, Y.; et al. Research and development of liquid hydrogen (LH2) temperature monitoring system for marine applications. *Int. J. Hydrogen Energy* **2021**, *46*, 15649–15659. [CrossRef]

95. Farber, E. The Development of Metal Hydride Chemistry. *Chymia* **1962**, *8*, 165–180. [CrossRef]

96. Førde, T.; Næss, E.; Yartys, V.A. Modelling and experimental results of heat transfer in a metal hydride store during hydrogen charge and discharge. *Int. J. Hydrogen Energy* **2009**, *34*, 5121–5130. [CrossRef]

97. Energ, A. Manual de Instalación y Uso de Hidruros Metálicos HBOND1500.

98. Bhattacharyya, R.; El-Emam, R.S.; Khalid, F. Multi-criteria analysis for screening of reversible metal hydrides in hydrogen gas storage and high pressure delivery applications. *Int. J. Hydrogen Energy* **2022**, *47*, 19718–19731. [CrossRef]

99. Tarasov, B.P.; Fursikov, P.V.; Volodin, A.A.; Bocharnikov, M.S.; Shimkus, Y.Y.; Kashin, A.M.; Yartys, V.A.; Chidziva, S.; Pasupathi, S.; Lototskyy, M.V. Metal hydride hydrogen storage and compression systems for energy storage technologies. *Int. J. Hydrogen Energy* **2021**, *46*, 13647–13657. [CrossRef]

100. Bellosta von Colbe, J.; Ares, J.-R.; Barale, J.; Baricco, M.; Buckley, C.; Capurso, G.; Gallandat, N.; Grant, D.M.; Guzik, M.N.; Jacob, I.; et al. Application of hydrides in hydrogen storage and compression: Achievements, outlook and perspectives. *Int. J. Hydrogen Energy* **2019**, *44*, 7780–7808. [CrossRef]

101. Moradi, R.; Groth, K.M. Hydrogen storage and delivery: Review of the state of the art technologies and risk and reliability analysis. *Int. J. Hydrogen Energy* **2019**, *44*, 12254–12269. [CrossRef]

102. Majzoub, E.H.; Rönnebro, E.C.E. Methodology of materials discovery in complex metal hydrides using experimental and computational tools. *Mater. Sci. Eng. R Reports* **2012**, *73*, 15–26. [CrossRef]

103. Milanese, C.; Jensen, T.R.; Hauback, B.C.; Pistidda, C.; Dornheim, M.; Yang, H.; Lombardo, L.; Zuettel, A.; Filinchuk, Y.; Ngene, P.; et al. Complex hydrides for energy storage. *Int. J. Hydrogen Energy* **2019**, *44*, 7860–7874. [CrossRef]

104. Ley, M.B.; Jepsen, L.H.; Lee, Y.-S.; Cho, Y.W.; Bellosta Von Colbe, J.M.; Dornheim, M.; Rokni, M.; Jensen, J.O.; Sloth, M.; Filinchuk, Y.; et al. Complex hydrides for hydrogen storage—New perspectives. *Mater. Today* **2014**, *17*, 122–128. [CrossRef]

105. Mcwhorter, S.; Read, C.; Ordaz, G.; Stetson, N. Materials-based hydrogen storage: Attributes for near-term, early market PEM fuel cells. *Curr. Opin. Solid State Mater. Sci.* **2011**, *15*, 29–38. [CrossRef]

106. Millet, P. Hydrogen storage in hydride-forming materials. In *Advances in Hydrogen Production, Storage and Distribution*; Woodhead Publishing: Sawston, UK, 2014; pp. 368–409. [CrossRef]

107. George, L.; Saxena, S.K. Structural stability of metal hydrides, alanates and borohydrides of alkali and alkali- earth elements: A review. *Int. J. Hydrogen Energy* **2010**, *35*, 5454–5470. [CrossRef]

108. Li, Z.P.; Liu, B.H.; Arai, K.; Asaba, K.; Suda, S. Evaluation of alkaline borohydride solutions as the fuel for fuel cell. *J. Power Sources* **2004**, *126*, 28–33. [CrossRef]

109. Renewable Energy Agency, Making the Breakthrough: Green Hydrogen Policies and Technology Costs. 2021. Available online: www.irena.org (accessed on 4 August 2022).